Dexamethasone and Glucocorticoid-Induced Matrix Temporally Modulate Key Integrins, Caveolins, Contractility, and Stiffness in Human Trabecular Meshwork Cells

Felix Yemanyi,[1] Hasna Baidouri,[1] Alan R. Burns,[1] and VijayKrishna Raghunathan[1,2]

[1]Department of Basic Sciences, University of Houston College of Optometry, Houston, Texas, United States
[2]Department of Biomedical Engineering, Cullen College of Engineering, University of Houston, Houston, Texas, United States

Correspondence: VijayKrishna Raghunathan, Department of Basic Sciences, University of Houston College of Optometry, 4901 Calhoun Road, Houston, TX 77204, USA; vraghunathan@uh.edu.

Received: April 17, 2020
Accepted: October 16, 2020
Published: November 10, 2020

Citation: Yemanyi F, Baidouri H, Burns AR, Raghunathan V. Dexamethasone and glucocorticoid-induced matrix temporally modulate key integrins, caveolins, contractility, and stiffness in human trabecular meshwork cells. *Invest Ophthalmol Vis Sci.* 2020;61(13):16. https://doi.org/10.1167/iovs.61.13.16

Purpose. To determine the temporal effects of dexamethasone (DEX) and glucocorticoid-induced matrix (GIM) on integrins/integrin adhesomes, caveolins, cytoskeletal-related proteins, and stiffness in human trabecular meshwork (hTM) cells.

Methods. Primary hTM cells were plated on plastic dishes (TCP), treated with vehicle (Veh) or 100 nM DEX in 1% serum media for 1, 3, 5, and 7 day(s). Concurrently, hTM cells were also plated on vehicle control matrices (VehMs) and GIMs for similar time points; VehMs and GIMs had been generated from chronic cultures of Veh-/DEX-stimulated hTM cells and characterized biochemically. Subsets of cells prior to plating on TCP or VehMs / GIMs served as baseline. Protein expression of mechanoreceptors, cytoskeletal-related proteins, and elastic moduli of hTM cells were determined.

Results. Compared with Veh, DEX temporally overexpressed αV, β3, and β5 integrins from day 3 to day 7, and integrin linked kinase at day 7, in hTM cells. However, DEX decreased β1 integrin at day 1 and day 7, while increasing Cavin1 at day 7, in a time-independent manner. Further, DEX temporally upregulated α-smooth muscle actin(α-SMA) and RhoA at day 7 and day 5, respectively; while temporally downregulating Cdc42 at day 3 and day 7 in hTM cells. Conversely, GIM showed increased immunostaining of fibronectin extra-domain A and B isoforms. Compared with VehM, GIM temporally increased αV integrin, Cavin1, and RhoA from day 3 to day 7, at day 3 and day 7, and at day 5, respectively, in hTM cells. Further, GIM overexpressed α-SMA at day 3 and day 7, and stiffened hTM cells from day 1 to day 7, in a time-independent fashion.

Conclusions. Our data highlight crucial mechanoreceptors, integrin adhesomes, and actin-related proteins that may temporally sustain fibrotic phenotypes precipitated by DEX and/or GIM in hTM cells.

Keywords: integrin, caveolin, extracellular matrix, mechanotransduction, biomechanics, Rho-GTPase

A better understanding of the molecular mechanisms underpinning ocular hypertension in glucocorticoid-induced glaucoma (GIG) is relevant for identification of hypotensive targets that would inform the design of novel therapeutics to serve at least two main purposes: First, to increase the vision-related quality of life of patients with GIG and primary open angle glaucoma (POAG). The latter is because cortisol levels are elevated in POAG[1–3] and mechanisms of ocular hypertension in POAG share similarities with GIG.[4–9] Second, to increase the benefit-to-risk ratio of the potent anti-inflammatory effects of glucocorticoids,[10–13] by ameliorating ocular hypertension as its major side effect among 30 to 40% of the normal population,[4,14–16] and over 90% of patients with POAG.[14,17–19] Consequently, dexamethasone (DEX), which is a potent glucocorticoid, has been used as a glaucomatous stimulus in several mechanistic investigations to document aberrant remodeling of trabecular meshwork (TM) cells, or their extracellular matrix (ECM), or both.[20] The primary egress for aqueous humor is the TM, whose pathobiology is the main cause of increased obstruction to aqueous outflow, and subsequent ocular hypertension.[21–24]

Examples of DEX-induced TM cell remodeling implicated in ocular hypertension[25–27] are increased contractility,[28] increased formation of crosslinked actin networks (CLANs),[29–32] increased stiffness,[7] impaired phagocytosis,[33–35] and endoplasmic reticulum stress,[27,36] to mention but a few. On the other hand, DEX-induced ECM remodeling deemed responsible for increased resistance to aqueous outflow encompasses aberrant changes to its

structural, matricellular, crosslinking, and turnover components typically resulting in increased ECM deposition and/or stiffness.[7,25,36–43] Specific cell-matrix mechanoreceptors, like integrin subunits/integrin adhesomes[38,44–46] and caveolins,[32,47] and key intracellular cytoskeletal-related proteins,[48–53] have been identified as critical mediators in these DEX-induced TM cell and/or ECM changes. For instance, $\beta1$,[52,54,55] $\beta3$,[30,40,54] and $\alpha V\beta3$[40,46,56] integrins, and integrin linked kinase[44] have all been implicated in aberrant remodeling of the actin cytoskeleton (such as CLANs formation) and/or ocular hypertension. Similarly, membrane-bound cave-like structures, caveolae, have been implicated in fibrotic phenotypes, ECM remodeling, autophagy, and ocular hypertension.[32,47,57–59] Moreover, cytoskeletal-related proteins, like RhoA,[49,51] Cdc42,[48] Rac 1/2/3,[50] and intermediate filament vimentin,[52,53,60] typically downstream of integrins and caveolae,[45,61–63] have also been implicated in fibrotic phenotypes.[64,65] However, most of these studies either focused on only few crucial mechanoreceptors and cytoskeletal-related proteins at any given time or performed experiments at a single/limited time point(s). Further, clinically, about 1 to 3% of the 30 to 40% steroid responders still have ocular hypertension despite steroid cessation.[17,66,67] In support of this observation, Faralli and colleagues[46] showed sustained elevation of the ocular hypertensive protein, $\beta3$ integrin,[56] in hTM cells for up to 2 weeks even after DEX removal. Recently, we demonstrated that, in the absence of exogenous DEX, glucocorticoid-induced matrix (GIM) triggers POAG-associated non-Smad transforming growth factor $\beta2$ (TGF$\beta2$) signaling, correlated with aberrant changes in target ECM genes and proteins in human TM (hTM) cells.[68] Therefore, we hypothesized that, in the absence of the primary insult, the pathological consequences of DEX on the ECM (that is, GIM) partly sustains ocular hypertensive phenotypes in hTM cells in a time-dependent fashion. There is mounting evidence that integrins, caveolins, and cytoskeletal-related proteins modulate in response to biomechanical cues like stretching and/or substrate stiffness;[58,61,69–73] GIMs are stiffer than their vehicle control matrices (VehMs),[7] and, therefore, cannot be an exception.

Thus, because POAG is a chronic disease and aqueous homeostasis by the TM is a dynamic process,[23,74,75] first, we determined the time-dependent effect of DEX (together with its vehicle control [Veh]) on the protein expression of specific integrin subunits/integrin adhesomes, caveolins, and cytoskeletal-related proteins concurrently in hTM cells. Second, we repeated the same for GIM (and its vehicle control, VehM) in the absence of any additional DEX, adding cellular biomechanics as an outcome measure.

Materials and Methods

Trabecular Meshwork Tissue Dissection and Concomitant Cell Culture

Primary hTM cells were carefully isolated from donor corneoscleral rims (age range of donors was between 48 and 75 years) unsuitable for transplant (SavingSight Eye Bank, St. Louis, MO, USA) with no known history of ocular disease or trauma, as previously described.[76] All primary hTM cell strains used in this study were validated with DEX-induced expression of myocilin in compliance with consensus recommendation for hTM cell culture.[76] Further, hTM cells were generally utilized between passages two (2) and six (6). This study is institutional review board (IRB) exempt and not considered human subject research because cells were acquired postmortem from de-identified donor tissues. Nevertheless, all experiments were done in compliance with the tenets of the Declaration of Helsinki.

Treating hTM Cells Cultured on Plastics With DEX Paralleled With Seeding Cells on VehM and GIM Without Further Treatment

Two distinct experiments were simultaneously performed in this study. In the first set of experiments, primary hTM cells cultured on tissue culture plastic dishes (5,000–10,000 per cm^2) were treated with vehicle control or DEX (100 nM) in 1% fetal bovine serum (FBS) growth media for 1, 3, 5, and 7 day(s). We cultured cells in 1% FBS growth media in order to minimize confounding effects of endogenous growth factors that may be present in serum while ensuring cell survival. In the second set of experiments, primary hTM cells from the same donor, as those used to generate matrices, were seeded on VehMs and GIMs at early passages (5,000–10,000 per cm^2; referred to as recellularization) in 1% FBS growth media without further treatments for similar time points as with the first experiment. Subsets of hTM cells that were detached from routine T75 culture plastics prior to plating on plastic substrates or VehMs / GIMs served as baseline (considered time point 0 day) for protein normalization across time points. Subsequently, hTM cells from these two distinct experiments were lysed at the end of each time point and protein isolated for Western blotting. Immunocytochemistry (for cell-ECM interaction) and transmission electron microscopy (to visualize caveolae) were performed. We have documented a comprehensive protocol for troubleshooting, generating and characterizing VehMs and GIMs from cultured hTM cells elsewhere.[77] Herein, we briefly describe the steps involved below.

Generating VehM and GIM from Cultured hTM Cells

Primary hTM cells were seeded on sterile pretreated 60 mm dishes (5,000–10,000 cells per cm^2) and aminosilane-modified 12 mm glass coverslips (to enhance robust attachment of deposited ECM to glass substrate)[7,78] in a 24-well culture plate (5,000–10,000 cells per cm^2) using complete growth media. When the cultured cells were approximately 80 to 90% confluent, they were stimulated with 100 nM DEX (DEX; Sigma-Aldrich Corp., St. Louis, MO, USA) or its vehicle control, ethanol (EtOH), for 4 weeks with media changes done on every other day. Subsequently, hTM cells were removed using 20 mM ammonium hydroxide, 0.05% Triton X-100, and deionized water as solvent to obtain VehMs or GIMs.[7,77,79] These cell-derived matrices (CDMs)[77] were subsequently treated with 50 U/mL DNase I and RNase A for 2 hours, and then washed thoroughly in Hank's balanced salt solution (HBSS) prior to subsequent immunocytochemistry and cell culture. Immunocytochemistry was done to determine localization of key ECM structural proteins (for example, fibronectin and collagen IV), whereas confirming complete removal of any resident cellular material.

Investigative Ophthalmology & Visual Science

Table. Antibodies for Western Blotting Analyses

Antibody	Catalog Number	Stock Concentration, µg/mL	Dilution	Final Concentration, µg/mL	Source
FKBP5	12210	918.0	1/5000	0.184	Cell Signaling Technology, Danvers, MA, USA
αV Integrin	4711	53.0	1/2000	0.027	
β1 Integrin (D2E5)	9699	100.0	1/5000	0.020	
β3 integrin (D7X3P) XP	13166	66.0	1/5000	0.013	
β5 integrin (D24A5)	3629	338.0	1/5000	0.068	
Focal adhesion kinase	3285	31.0	1/2000	0.016	
Phospho-focal adhesion kinase	8556	16.0	1/2000	0.008	
Integrin linked kinase	3856	458.0	1/5000	0.092	
Caveolin1	3267	689.0	1/5000	0.138	
Cavin1	46379	30.0	1/5000	0.006	
Cdc42	2462	585.0	1/5000	0.117	
Rac1/2/3	2465	39.0	1/5000	0.008	
RhoA	2117	107.0	1/5000	0.021	
Vimentin	5741	45.0	1/5000	0.009	
β-Actin	4970	61.0	1/10000	0.006	
α-SMA	A5228	2000.0	1/5000	0.400	Sigma-Aldrich, St. Louis, MO, USA
Goat anti-Rabbit IgG (H + L) Cross-Adsorbed Secondary Antibody, HRP	G-21234	1000.0	1/10000	0.100	Invitrogen, Carlsbad, CA, USA
Goat anti-Mouse IgG (H + L) Cross-Adsorbed Secondary Antibody, HRP	G-21040	1000.0	1/10000	0.100	

Immunocytochemistry for Decellularized and Recellularized VehMs and GIMs

Decellularized and recellularized VehMs and GIMs on glass coverslips were fixed in 4% paraformaldehyde in phosphate buffered solution (PBS) at 4°C for 30 minutes, washed 3 times, 5 minutes each with PBS afterward; permeabilized with 0.25% Triton X-100 in PBS (where applicable) for 10 minutes, and washed 3 times, each for 5 minutes. Samples were subsequently blocked in 5% bovine serum albumin (BSA) in PBS for 30 minutes. Afterward, they were incubated overnight at 4°C with the following primary antibodies; Anti-Fibronectin (catalog number: ab6584; Abcam, Cambridge, MA, USA), anti-fibronectin extra domain A (ED-A; catalog number: ab6328; Abcam), anti-fibronectin extra domain B (ED-B; catalog number: ab154210; Abcam), anti-collagen IV (catalog number: ab6311; Abcam), respectively, at 1/250 dilution in 5% BSA/PBS (primary antibodies were omitted as negative controls; data not shown). After three 5-minute washes in PBS the following day, incubation was done with species-appropriate fluorophore-tagged secondary antibodies (Alexa Fluor 488 Anti-Rabbit and Anti-Mouse; Thermo Fisher Scientific) and CF594-conjugated Phalloidin (catalog number: 00045; Biotium, Fremont, CA, USA) at 1/500 dilution in room temperature for 1 hour. Following three 5-minute washes, samples were counterstained with 4′6-diamidino-2-phenylindole (DAPI; catalog number: D1306; Fisher Scientific, Petaluma, CA, USA) at 1/10,000 dilution for 5 minutes. After one 5-minute wash, glass coverslips were mounted with Fluoromount-G Mounting Medium (catalog number: 0100-01; Southern Biotech, Birmingham, AL, USA) onto slides. Immunofluorescent images were then captured with Zeiss LSM 800 laser scanning confocal microscope (Carl Zeiss, Jena, Germany) with a 20 times objective. For each immunolabelled glass coverslip, 5 to 10 random locations were imaged. At least three glass coverslips were used for each immunolabeling condition for each cell strain with the same imaging settings for all cohorts.

Protein Extraction and Western Blot Analysis

Protein extraction was done in two phases: (i) primary hTM cells, prior to plating on plastic substrates or VehMs / GIMs, were detached using trypsin, and (ii) primary hTM cells that had first been detached using trypsin and subsequently plated on plastic substrates with Veh / DEX treatment, or plated on VehMs / GIMs without any further treatment, were, respectively, lysed and scraped into radioimmunoprecipitation assay (RIPA) buffer (Thermo-Scientific, Waltham, MA, USA) supplemented with protease and phosphatase inhibitors (Fisher Scientific, Hampton, NH, USA) on ice at each time point (that is, 1, 3, 5, and 7 day[s]). Subsequently, cell lysates were centrifuged at 12,000 g for 15 minutes at 4°C; any cellular debris pelleted was excluded. Supernatants were transferred to new tubes and quantified by a modified Lowry assay (DC assay; Biorad, Hercules, CA, USA) with BSA as the standard. Next, protein lysates were denatured in a 1:10 mixture of 2-mercaptoethanol and 4 times Laemmli buffer by boiling at 100°C for 5 minutes. Following an immediate centrifuge of the denatured proteins at 15,000 g for 30 seconds, equal amounts of protein (20 µg) were loaded per well for each sample and ran on denaturing 4 to 15% gradient polyacrylamide ready-made gels (Biorad); subsequently transferred onto polyvinylidene difluoride (PVDF) membranes by electrophoresis. Membrane blots were blocked in 5% BSA in 1 times tris buffered saline / tween-20 (TBST) for 1 hour. Immunoblots were then incubated overnight at 4°C with specific primary antibodies (Table) on a shaker. The membrane blot was washed 3 times with TBST; each wash lasting for about 10 minutes. Subsequent incubation with

Investigative Ophthalmology & Visual Science

corresponding horse radish peroxidase (HRP)-conjugated species-specific secondary antibodies (Table) for 45 minutes was done, followed by three 10-minute washes with TBST. Protein bands were visualized using ECL detection reagents (SuperSignal West Femto Maximum Sensitivity Substrate; Life Technologies, Grand Island, NY, USA) and imaged with a Bio-Rad ChemiDoc MP imaging system. Respective membrane blots were stripped and probed with β-Actin as a loading control. Densitometric analysis was performed using ImageJ.

Visualizing Caveolae in Cells Cultured on VehMs and GIMs

Primary hTM cells cultured on VehMs and GIMs for 7 days were fixed (using 2.5% glutaraldehyde in 0.1M sodium cacodylate with calcium chloride) at room temperature for 1 hour and scraped for post-fixation in 1% osmium tetroxide followed by dehydration in an acetone series. Samples were embedded in Embed 812 resin, ultra-thin sections cut, and collected on formvar-coated grids. Transmission electron microscopy was performed to visualize caveolae.

Measuring Biomechanics of hTM Cells on VehMs and GIMs Via Atomic Force Microscopy

Biomechanics of hTM cells seeded on VehMs and GIMs at 1, 3, 5, and 7 day(s) was determined via atomic force microscopy as described previously.[7,74,78,80,81] Briefly, PNP-TR cantilever with a conical tip (nominal spring constant 0.32 N/m; Nano and More, Watsonville, CA, USA) was used without any modification. After calibration and equilibration of samples in HBSS for 30 minutes, at least 5 force-distance curves were obtained in contact mode for 10 random cells. Data were subsequently analyzed using a custom semi-automated Matlab program to determine elastic moduli using analytical principles previously described[82] (for example, automatically restricting cantilever's indentation to the linear elastic region of the biologic sample using a Poisson ratio of 0.5 for incompressible biologic samples and a Sneddon model) with slight modification (for instance, subjectively identifying contact point for each force curve).

Statistics

To document temporal changes in the expression of proteins, data in respective groups (that is, Veh, DEX, VehM, and GIM) were normalized to baseline protein levels (at time point 0 day), with β-actin as a housekeeping protein. Then, congruent with our hypothesis / purpose, 2-way ANOVA followed by Holm-Sidak multiple comparisons post hoc test was used for analysis between (for instance, Veh versus Dex or VehM versus GIM) and within (for example, Veh or VehM relative to baseline proteins) groups, with P values < 0.05 considered to be statistically significant. Similarly, 2-way ANOVA was used to establish time-dependent changes in cell biomechanics between VehM and GIM. All data are presented as mean $\pm$ standard error of the mean (SEM; $n =$ 3–5 biological replicates) in bar graphs, cello plots, representative confocal/transmission electron micrographs, and blots where applicable.

Results

DEX or Veh Temporally and Differentially Modulated Expression of Specific Integrin Subunits, Integrin Adhesomes, and Caveolins in hTM Cells

Given the important role of integrins as transmembrane heterodimers implicated in cell-ECM interactions,[40,45,83] we determined whether Veh-induced or DEX-induced expression of specific integrin subunits in hTM cells was dependent on time. We also dwelled on the temporal expression of specific integrin adhesomes owing to their cytoplasmic activation of integrins.[73,84,85] We found that the effect of Veh or DEX on the expression of αV integrin significantly depended on time ($F[4, 40] = 4.532$, $P = 0.0041$), with treatment-time interaction accounting for 13.24% of the total variance. Compared with Veh, post hoc analysis revealed DEX markedly sustained overexpression of αV integrin ($P < 0.01$, $P < 0.01$, and $P < 0.001$, respectively) from day 3 to day 7 in hTM cells. Veh did not have any significant effect on αV integrin in hTM cells relative to baseline protein levels (Fig. 1A). In addition, there was no significant interaction between treatment and time with regard to β1 integrin's expression in hTM cells. However, treatment alone or time alone had a significant main effect on expression of β1 integrin ($F[1, 40] = 18.83$, $P = 0.0001$ and $F[4, 40] = 11.52$, $P = 0.0001$, respectively), accounting for 16.95% and 41.47% of respective total variances. Post hoc analysis revealed that, compared with Veh, DEX downregulated β1 integrin ($P < 0.05$, respectively) on days 1 and 7 in hTM cells. Compared with baseline proteins, whereas Veh significantly overexpressed β1 integrin from day 1 to day 7 ($P < 0.001$, $P < 0.05$, $P < 0.001$, and $P < 0.001$, respectively) in hTM cells, DEX markedly increased its expression on day 7 (Fig. 1B). Further, Veh- or DEX-mediated expression of β3 integrin in hTM cells was markedly dependent on time ($F[4, 40] = 30.37$, $P = 0.0001$), with treatment-time interaction being responsible for 26.01% of the total variance. Post hoc analysis showed that, compared with Veh, DEX significantly and permanently upregulated β3 integrin ($P < 0.001$, respectively) from day 3 to day 7. Compared with baseline proteins, Veh markedly downregulated β3 integrin ($P < 0.05$, $P < 0.01$, $P < 0.01$, and $P < 0.05$, respectively) from day 1 to day 7 in hTM cells (Fig. 1C). Moreover, the impact of Veh or DEX on the expression of β5 integrin significantly depended on time ($F[4, 40] = 22.08$, $P = 0.0001$), with treatment-time interaction accounting for 22.19% of the total variance. Compared with Veh, post hoc analysis revealed DEX significantly sustained overexpression of β5 integrin ($P < 0.001$, respectively) from day 3 to day 7 in hTM cells. Veh-induced expression of β5 integrin was not any different from baseline proteins (Fig. 1D). Similarly, Veh- or DEX-mediated expression of integrin linked kinase (ILK) in hTM cells was significantly dependent on time ($F[4, 40] = 2.622$, $P = 0.0489$), with treatment-time interaction accounting for 8.25% of the total variance. Post hoc analysis revealed that, compared with Veh, DEX markedly upregulated ILK ($P < 0.001$, respectively) on day 7 in hTM cells. Compared with baseline proteins, Veh significantly increased ILK ($P < 0.05$) on day 7 in hTM cells (Fig. 1E). Furthermore, no significant interaction between treatment and time was observed for focal adhesion kinase (FAK) in hTM cells. However, treatment alone or time alone had a marked main effect on FAK ($F[1, 40] = 7.188$, $P = 0.0106$ and $F[4, 40] = 7.193$,

Investigative Ophthalmology & Visual Science

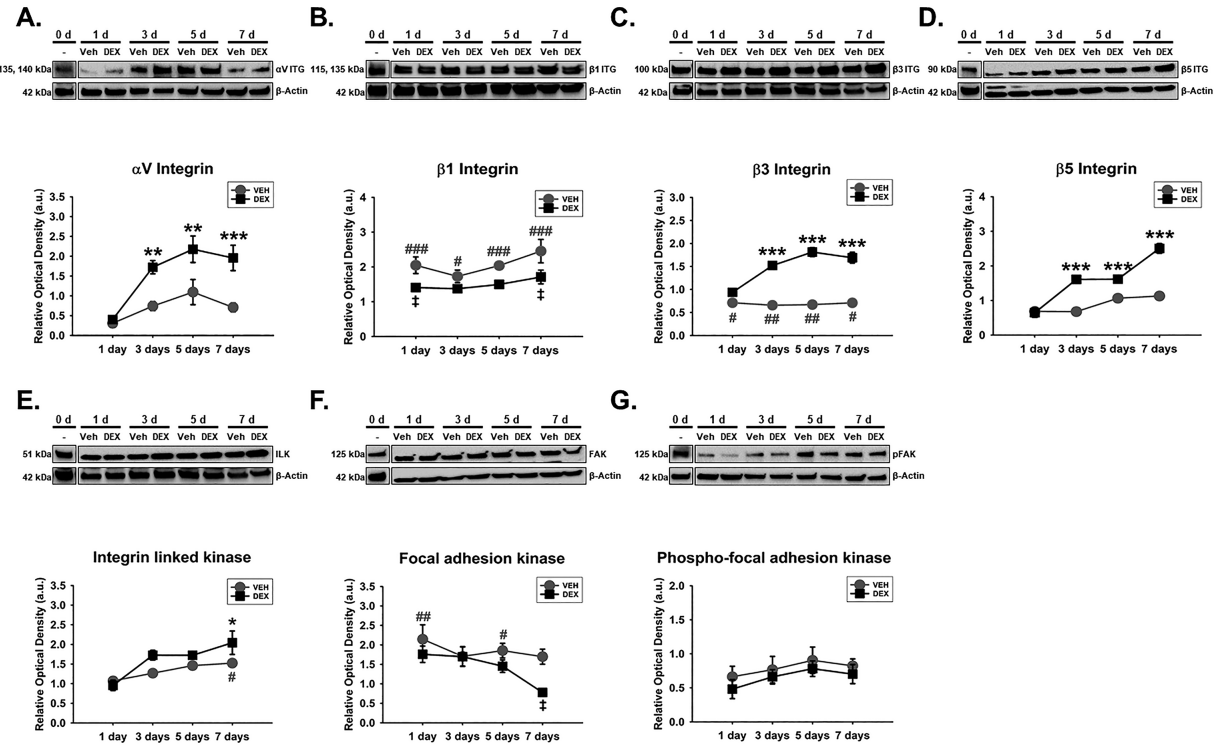

Figure 1. DEX or Veh temporally and differentially modulated specific integrin subunits and integrin adhesomes in hTM cells. Primary hTM cells were cultured on tissue culture plastics and treated with vehicle control (Veh) or 100 nM dexamethasone (DEX) in 1% FBS for 1, 3, 5, and 7 day(s). Protein was extracted for Western blot analysis. Veh and DEX were, respectively, normalized to baseline protein levels (time point 0 day). β-Actin was used as a housekeeping protein. Respective representative blot (*top*) and densitometric analysis (*bottom*) of (**A**) αV integrin, (**B**) β1 integrin, (**C**) β3 integrin, (**D**) β5 integrin, (**E**) integrin linked kinase, (**F**) focal adhesion kinase, and (**G**) phospho-focal adhesion kinase. *Columns and error bars*; means and standard error of mean (SEM). Two-way ANOVA with the Holm Sidak pairwise comparisons post hoc test was used for statistical analysis ($n = 5$ biological replicates). *$P < 0.05$, **$P < 0.01$, ***$P < 0.001$ for DEX versus Veh, given significant treatment and time interaction. ‡$P<0.05$ for DEX versus Veh, given significant main effect of treatment. #$P < 0.05$, ##$P < 0.01$, ###$P < 0.001$ for Veh versus Baseline protein. hTM, human trabecular meshwork.

$P = 0.0002$, respectively), accounting for 8.67% and 34.7% of respective total variances. Post hoc analysis revealed that, compared with Veh, DEX markedly downregulated FAK on day 7. Compared with baseline proteins, whereas Veh significantly increased FAK on days 1 and 5, DEX was not any different (Fig. 1F). Finally, whereas there was no significant main effect of treatment alone or its interaction with time regarding the expression of phosphorylated FAK (pFAK) in hTM cells, time alone had a significant main effect ($F[4, 40] = 2.884$, $P = 0.0345$; Fig. 1G).

Caveolae have emerged important regulators of aqueous humor homeostasis and ocular hypertensive phenotypes[47,57,58] owing to their cellular functions in endocytosis,[57,59] mechanotransduction,[71,72,86] actin cytoskeletal dynamics,[62] and ECM regulation[57] to mention but a few. Because Caveolin1 and Cavin1, which are critical components of caveolae,[87] could interact with integrins[70] and actin cytoskeleton,[62,63] next, we determined the temporal effects of Veh and DEX on these molecules in hTM cells. We observed that there was no significant main effect of treatment or its interaction with time regarding expression of Caveolin1 in hTM cells. However, Caveolin1's expression was significantly dependent on time ($F[4, 40] = 11.81$, $P = 0.0001$), with 51.51% accounting for the total variance (Fig. 2A). Furthermore, there was no significant interaction between treatment and time with regard to Cavin1's expression in hTM cells. However, treatment alone or time alone had a significant main effect on expression of Cavin1 ($F[1, 40] = 15.23$, $P = 0.0004$ and $F[4, 40] = 31.61$, $P = 0.0001$, respectively), accounting for 8.03% and 66.62% of respective total variances. Post hoc analysis revealed that, compared with Veh, DEX markedly upregulated Cavin1 on day 7 ($P < 0.01$) in hTM cells. Compared with baseline proteins, whereas Veh significantly overexpressed Cavin1 from day 5 to day 7 ($P < 0.01$, respectively) in hTM cells, DEX markedly increased its expression from day 3 to day 7 ($P < 0.05$, $P < 0.001$, and $P < 0.001$, respectively; Fig. 2B).

DEX or Veh Temporally and Differentially Modulated Specific Cytoskeletal-Related Proteins in hTM Cells

Considering that cytoskeletal dynamics are typically downstream of integrin- and/or caveolae-dependent signaling/mechanotransduction,[45,61–63] we subsequently determined the expression of specific actin-related proteins like α-SMA and Rho GTPases (specifically, Rac 1/2/3, Cdc42, and RhoA), which regulate actin cytoskeletal dynamics. We also looked at intermediate filament vimentin which has also been implicated in fibrotic phenotypes.[52,53] We found that

Investigative Ophthalmology & Visual Science

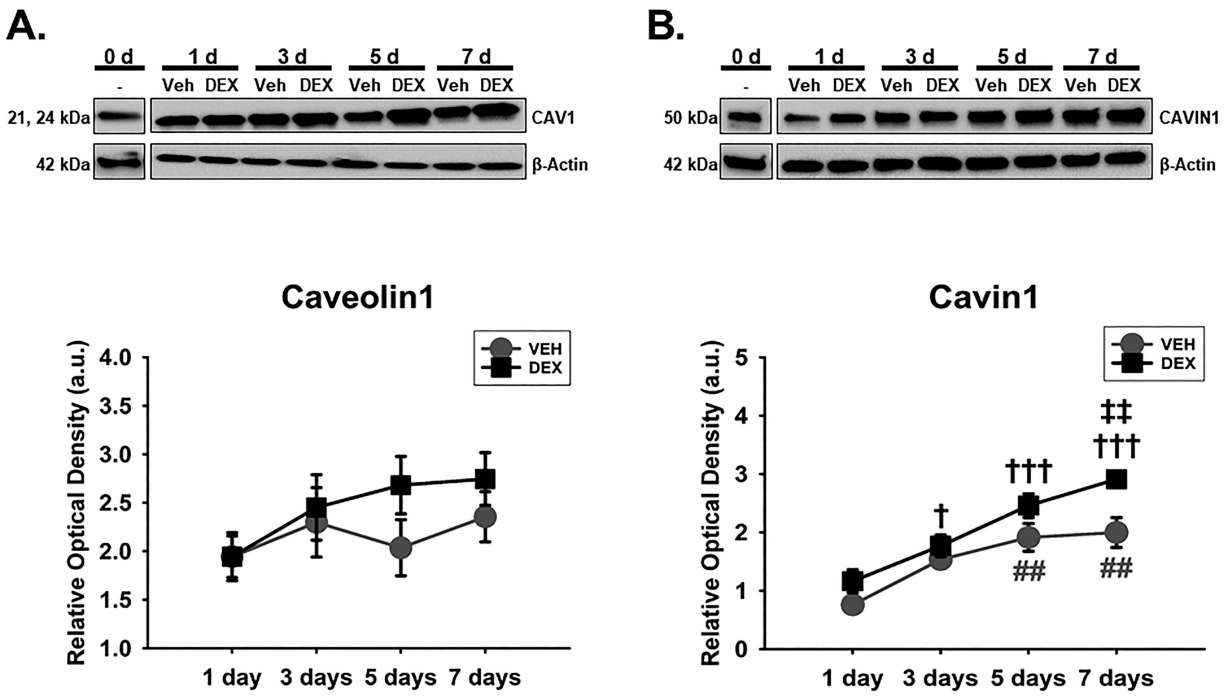

Figure 2. DEX or Veh temporally and differentially modulated Caveolin1 and Cavin1, major components of caveolae. Primary hTM cells cultured on tissue culture plastics were treated with vehicle control (Veh) or 100 nM dexamethasone (DEX) in 1% FBS for 1, 3, 5, and 7 day(s). Protein was extracted for Western blot analysis. Veh and DEX were each normalized to baseline protein levels (time point 0 day). β-Actin was used as an internal control. Respective representative blot (*top*) and densitometric analysis (*bottom*) of (**A**) Caveolin1 and (**B**) Cavin1. *Columns and error bars*; means and standard error of mean (SEM). Two-way ANOVA with the Holm Sidak pairwise comparisons post hoc test was used for statistical analysis ($n = 5$ biological replicates). $^{\ddagger\ddagger}P < 0.01$ for DEX versus Veh, given significant main effect of treatment. $^{\dagger}P < 0.05$, $^{\dagger\dagger\dagger}P < 0.001$ for DEX versus baseline proteins given significant main effect of treatment. $^{\#\#}P < 0.01$ for Veh versus baseline protein. hTM, human trabecular meshwork.

Veh- or DEX-induced expression of α-SMA in hTM cells was markedly dependent on time ($F[4, 40] = 10.49$, $P = 0.0001$), with treatment-time interaction accounting for 11.41% of the total variance. Post hoc analysis showed that, compared with Veh, DEX markedly overexpressed α-SMA ($P < 0.001$, respectively) on day 7. Compared with baseline proteins, Veh and DEX markedly increased α-SMA (Veh: $P < 0.01$, and $P < 0.001$; DEX: $P < 0.001$, respectively) from day 5 to day 7, respectively, in hTM cells (Fig. 3A). In addition, the effect of Veh or DEX on the expression of RhoA significantly depended on time ($F[4, 40] = 5.205$, $P = 0.0018$), with treatment-time interaction accounting for 14.95% of the total variance. Post hoc analysis showed that, compared with Veh, DEX significantly overexpressed RhoA ($P < 0.05$) in hTM cells on day 5, and decreased its expression ($P < 0.05$) on day 7. Compared with baseline proteins, whereas Veh significantly overexpressed RhoA ($P < 0.001$) on day 7 in hTM cells, DEX was not any different (Fig. 3B). Similarly, Veh- or DEX-induced expression of Rac 1/2/3 in hTM cells was significantly time-dependent ($F[4, 40] = 3.824$, $P = 0.0101$), with treatment-time interaction being responsible for 12.29% of the total variance. Post hoc analysis showed that, compared with baseline proteins, whereas Veh markedly decreased Rac 1/2/3 ($P < 0.001$ and $P < 0.01$, respectively) on days 1 and 5, DEX significantly downregulated its expression from day 1 to day 3 ($P < 0.0.001$, respectively; Fig. 3C). Further, the impact of Veh or DEX on the expression of Cdc42 was dependent on time ($F[4, 40] = 2.877$, $P = 0.0348$); interaction between treatment and time accounted for 16.09% of the total variance. Post hoc analysis showed that, compared with Veh, DEX markedly downregulated Cdc42 ($P < 0.01$, respectively) on days 3 and 7, respectively, in hTM cells (Fig. 3D). Finally, Veh- and Dex-mediated expression of vimentin was time-independent. However, treatment alone or time alone had a significant main effect on vimentin's expression ($F[1, 40] = 6.78$, $P = 0.0129$ and $F[4, 40] = 65.88$, $P = 0.0001$, respectively) in hTM cells. Compared with baseline proteins, Veh and DEX significantly decreased vimentin ($P < 0.001$, respectively) at all time points (Fig. 3E).

VehM and GIM Were Successfully Decellularized and Subsequently Recellularized

Before mirroring the time-dependent effect of Veh and DEX on specific mechanoreceptors, integrin adhesomes and cytoskeletal-related proteins in hTM cells, using VehM and GIM as stimulants (in the absence of any additional DEX added to the culture medium) and substrates for hTM cells, first, we demonstrate successful generation of respective VehMs (top horizontal panels) and GIMs (bottom horizontal panels) immunolabeled for two major ECM proteins, fibronectin (Fig. 4A) and collagen IV (Fig. 4B); with complete removal of resident cells (cytoplasmic indicator: Filamentous actin [F-actin]; nuclear material indicator: 4′,6-diamidino-2-phenylindole DAPI). In addition, we show cell-ECM

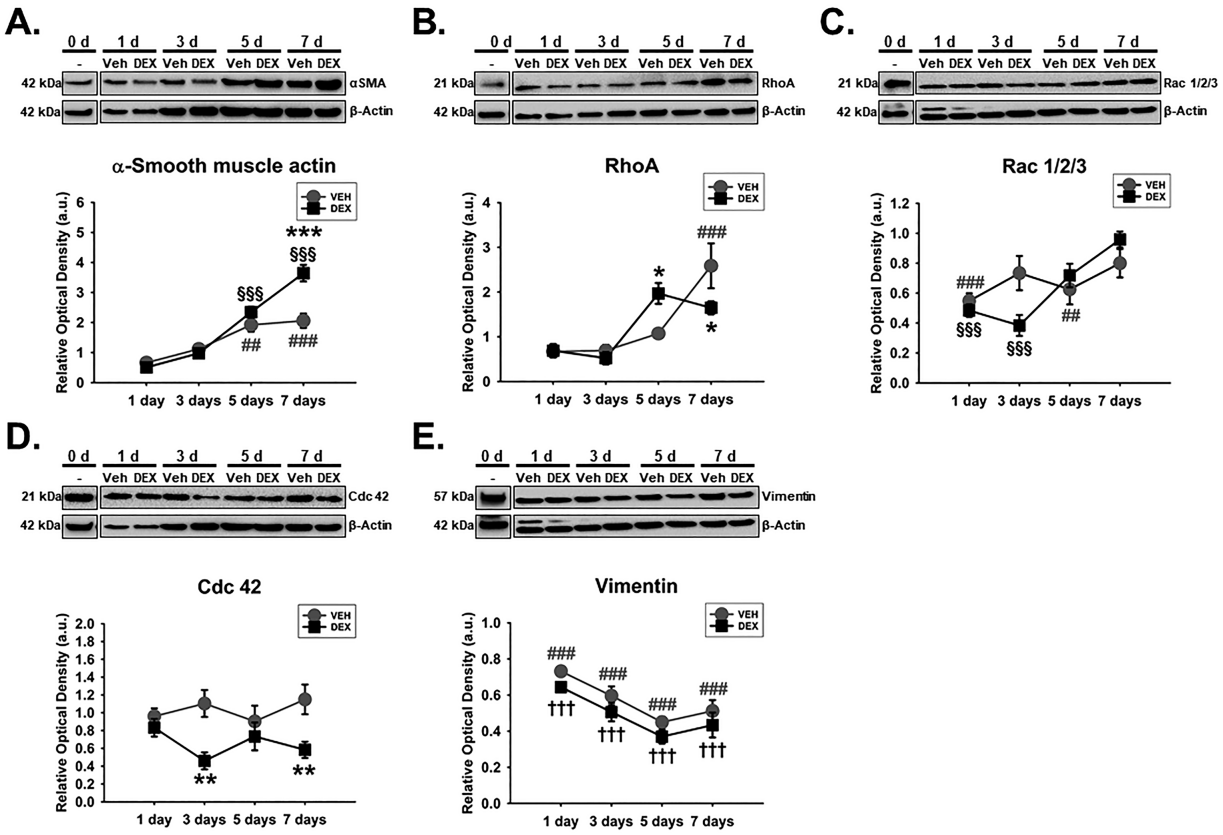

Figure 3. DEX or Veh temporally and differentially modulated key cytoskeletal proteins in hTM cells. Primary hTM cells were cultured on tissue culture plastics and treated with vehicle control (Veh) or 100 nM dexamethasone (DEX) in 1% FBS for 1, 3, 5, and 7 day(s). Protein was extracted for Western blot analysis. Veh and DEX were respectively normalized to baseline protein levels (time point 0 day). β-Actin was used as a housekeeping protein. Respective representative blot (*top*) and densitometric analysis (*bottom*) of (**A**) α-smooth muscle actin, (**B**) RhoA, (**C**) Rac 1/2/3, (**D**) Cdc 42, (**E**) vimentin. *Columns and error bars*; means and standard error of mean (SEM). Two-way ANOVA with the Holm Sidak pairwise comparisons post hoc test was used for statistical analysis ($n = 5$ biological replicates). $^{*}P < 0.05$, $^{**}P < 0.01$, $^{***}P < 0.001$ for DEX versus Veh, given significant treatment and time interaction. $^{§§§}P < 0.001$ for DEX versus baseline protein given significant treatment and time interaction. $^{†††}P < 0.001$ for DEX versus baseline protein given significant main effect of treatment. $^{\#\#}P < 0.01$, $^{\#\#\#}P < 0.001$ for Veh versus baseline proteins. hTM, human trabecular meshwork.

interactions with recellularized VehM and GIM immunolabeled for fibronectin (Fig. 4C).

GIM Showed Increased Immunolabeling of Fibronectin Extra Domain A and B Isoforms Compared With VehM

Next, given the wealth of evidence on the role of substratum properties in probably ligating with cells (for instance, via mechanoreceptors like integrins and/or caveolins) to influence their behavior,[69,80,88–94] we characterized decellularized VehMs and GIMs biochemically. In exploring probable ECM-dependent ligands, we focused on total fibronectin and two of its major isoforms, fibronectin extra domain A and B (FN ED-A and FN ED-B, respectively). Fibronectin's fibrillogenesis, FN ED-A, and FN ED-B have all been implicated in ocular hypertension and/or glaucoma.[40,95–98] As shown in Figures 5A and 5B, compared with respective VehMs (top horizontal panels), we observed GIMs (bottom horizontal panels) to demonstrate increased immunolabeling of FN ED-A and FN ED-B qualitatively, respectively, with the former appearing to be more pronounced.

GIM or VehM Temporally and Differentially Modulated Key Integrin Subunits, Integrin Adhesomes, and Caveolins in hTM Cells

Owing to the fact that ECM remodeling is intricately involved in the dynamics of aqueous homeostasis by the TM,[23,74,75] next, we determined the temporal expression of integrin subunits, integrin adhesomes, and caveolae in hTM cells, using VehMs and GIMs as substrate stimulants, in the absence of any additional DEX or Veh in the culture medium. We discovered that VehM- or GIM-mediated expression of αV integrin in hTM cells was significantly dependent on time ($F[4, 40] = 2.8$, $P = 0.0386$), with treatment-time interaction accounting for 6.74% of the total variance. Post hoc analysis revealed that, compared with VehM, GIM markedly and permanently overexpressed αV integrin ($P < 0.001$, $P < 0.05$, and $P < 0.001$, respectively) from day 3 to day 7. Compared with baseline proteins, VehM markedly decreased αV integrin ($P < 0.05$) on day 1 in hTM cells (Fig. 6A). Further, whereas there was no significant main effect of treatment or its interaction with time regarding the expression of β1 integrin in hTM cells, time had a significant main effect ($F[4, 40] = 11.99$, $P < 0.0001$), being responsible for 52.48% of the total variance. Compared with baseline proteins, VehM

Investigative Ophthalmology & Visual Science

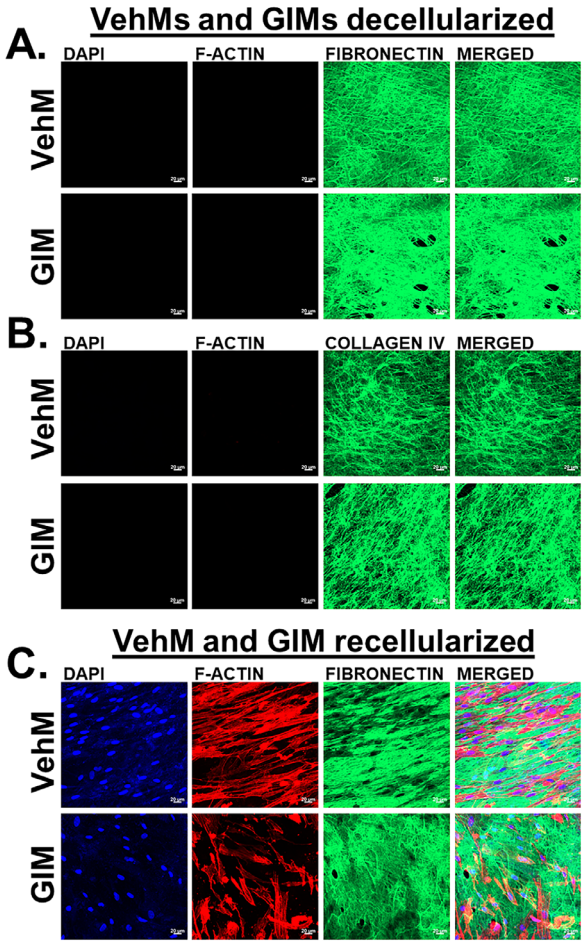

Figure 4. VehMs and GIMs successfully decellularized and recellularized. VehMs and GIMs were generated from primary hTM cells that had been cultured in the absence or presence of 100 nM dexamethasone (DEX), respectively, for 4 weeks. Primary hTM cells from the same donor used to generate these matrices were subsequently seeded on VehMs and GIMs in 1% fetal bovine serum (FBS) growth media for 7 days. Immunocytochemistry was subsequently performed. Representative confocal fluorescence micrographs of (**A**) decellularized VehMs (*top panel*) and GIMs (*bottom panel*) showing fibronectin, (**B**) decellularized VehMs (*top panel*) and GIMs (*bottom panel*) showing collagen IV, (**C**) recellularized VehMs (*top panel*) and GIMs (*bottom panel*) showing fibronectin. VehMs, vehicle control matrices. GIMs, glucocorticoid-induced matrices. hTM, human trabecular meshwork. Scale, 20 µm.

markedly decreased β1 integrin ($P < 0.01$) on day 1 in hTM cells (Fig. 6B). Further, there was no significant main effect of treatment or time or their interaction with regard to β3 integrin's expression in hTM cells (Fig. 6C). Moreover, there was no marked interaction between treatment and time with regard to β5 integrin's expression in hTM cells. However, treatment alone or time alone had a significant main effect on expression of β5 integrin (F[1, 40] = 7, $P = 0.0116$ and F[4, 40] = 7.436, $P = 0.0001$, respectively), being responsible for 8.79% and 37.35% of respective total variances. Post hoc analysis showed that, compared with baseline proteins, GIM upregulated β5 integrin ($P < 0.01$ and $P < 0.05$, respectively) on days 3 and 7 in hTM cells, whereas VehM was not any different (Fig. 6D). Furthermore, whereas there was no marked main effect of treatment or its interaction with time for the expression of ILK, time alone had a marked main effect on its expression (F[4, 40] = 4.496, $P < 0.0043$), accounting for 28.35% of the total variance (Fig. 6E). Further, there was no significant main effect of treatment or time or their interaction for the expression of FAK (Fig. 6F). Finally, whereas there was no main effect of treatment or its interaction with time for pFAK's expression in hTM cells, time alone had a marked main effect (F[4, 40] = 8.853, $P < 0.0001$); accounting for 51.92% of the total variance. Compared with baseline pFAK levels, VehM was not any different (Fig. 6G).

Next, we determined the effects of VehMs and GIMs on the expression of Caveolin1 and Cavin1 in hTM cells over time. We discovered that, whereas there was no significant main effect of treatment or its interaction with time for the expression of Caveolin1 in hTM cells, there was a significant main effect of time (F[4, 40] = 3.634, $P = 0.0129$), being responsible for 24.01% of the total variance. Compared with baseline proteins, VehM decreased Caveolin1 ($P < 0.05$) in hTM cells on day 5 (Fig. 7A). However, the VehM- or GIM-mediated expression of Cavin1 was significantly dependent on time (F[4, 40] = 3.541, $P = 0.0145$), with treatment-time interaction accounting for 13.84% of the total variance. Post hoc analysis revealed that, compared with VehM, GIM significantly overexpressed Cavin1 ($P < 0.05$ and $P < 0.001$, respectively) on days 3 and 7 in hTM cells (Fig. 7B). Further, as to whether hTM cells can form caveolae when cultured on matrices, for the first time, we showed that cells cultured on VehMs and GIMs do form these mechanosensitive membrane-bound cave-like structures (Figs. 7C, 7D, respectively).

GIM Temporally and Differentially Regulated Specific Cytoskeletal-Related Proteins in hTM Cells

We next determined the time-dependent effects of VehM and GIM on key cytoskeletal-related proteins in hTM cells. We observed that, whereas there was no significant interaction between treatment and time for the expression of α-SMA in hTM cells, treatment alone or time alone had a significant main effect on its expression (F[1, 40] = 11.92, $P = 0.0013$ and F[4, 40] = 2.677, $P = 0.0454$, respectively), being responsible for 17.14% and 15.39% of respective total variations. Subsequent post hoc analysis showed that, compared with VehM, GIM markedly increased α-SMA on days 3 and 7 ($P < 0.05$, respectively; Fig. 8A). Additionally, there was a significant interaction between treatment and time for RhoA's expression (F[4, 40] = 5.476, $P = 0.0013$) in hTM cells; accounting for 26.86% of the total variance. Post hoc analysis revealed that, compared with VehM, GIM markedly overexpressed RhoA ($P < 0.001$) in hTM cells transiently on day 5 (Fig. 8B). Further, whereas there was no marked main effect of treatment or its interaction with time for the expression of Rac 1/2/3 in hTM cells, time alone had a significant main effect on its expression (F[4, 40] = 2.793, $P = 0.0389$), being responsible for 19.81% of the total variation (Fig. 8C). Similarly, but for time alone (F[4, 40] = 4.992, $P = 0.0033$), which accounted for 33.95% of the total variance, interaction between treatment and time or treatment alone did not have any significant impact on Cdc 42's expression in hTM cells (Fig. 8D). Finally, there was no significant interaction between treatment and time or main effect of treatment alone or time alone on the expression of vimentin in hTM cells (Fig. 8E).

Investigative Ophthalmology & Visual Science

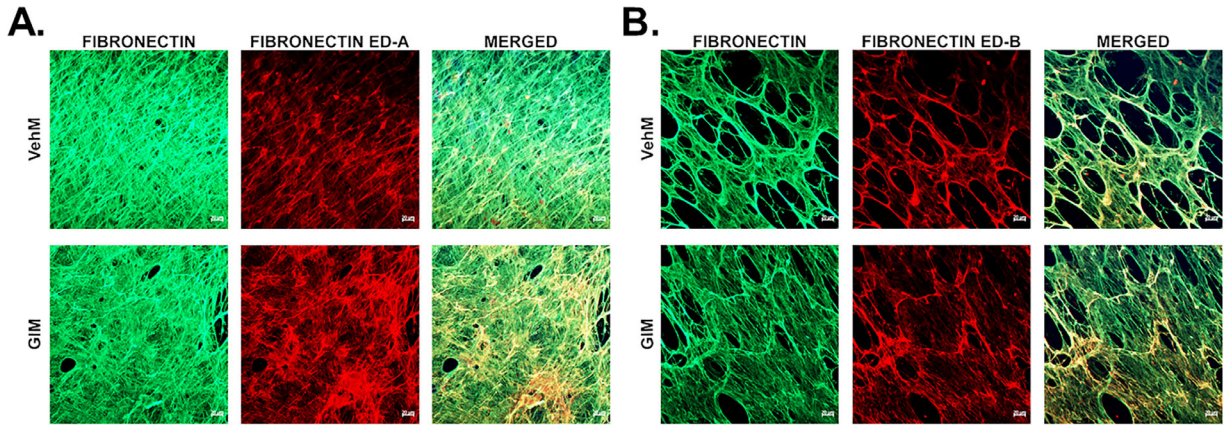

Figure 5. GIMs showed increased immunostaining of fibronectin ED-A and ED-B isoforms. Primary hTM cells were cultured in the absence or presence of 100 nM dexamethasone (DEX) in complete growth media for 4 weeks and decellularized to obtain VehMs and GIMs, respectively. Immunocytochemistry was performed. Representative confocal fluorescence micrographs of (**A**) total fibronectin and fibronectin extra domain A (ED-A), and (**B**) total fibronectin and fibronectin extra domain B (ED-B). hTM, human trabecular meshwork; VehMs, vehicle control matrices; GIMs, glucocorticoid-induced matrices. Scale, 20 µm.

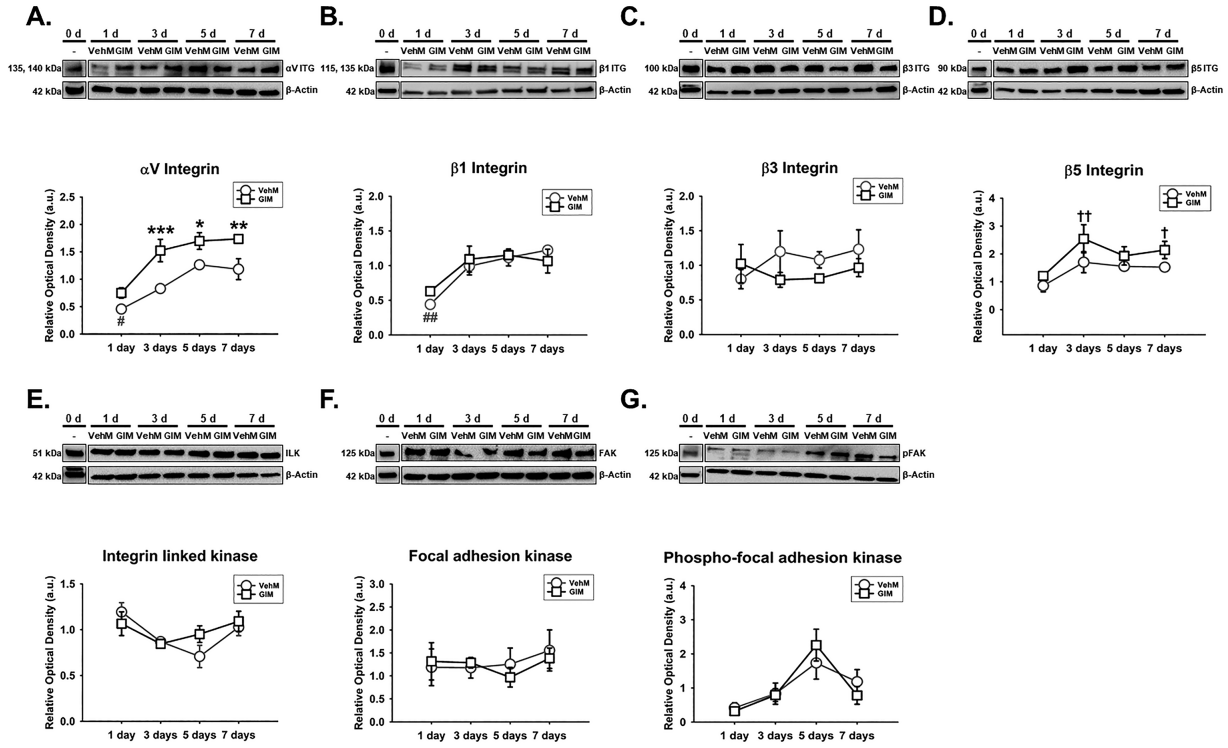

Figure 6. GIM or VehM temporally and differentially modulated specific integrin subunits and integrin adhesomes in hTM cells. Primary hTM cells were treated with vehicle control (Veh) or 100 nM dexamethasone (DEX) in complete growth media for 4 weeks and decellularized to obtain VehMs and GIMs. New hTM cells from the same donor used to generate these matrices were subsequently cultured on VehMs and GIMs in 1% fetal bovine serum (FBS) growth media for 1, 3, 5, and 7 day(s). Protein was extracted for Western blot analysis. VehM and GIM were respectively normalized to baseline protein levels (time point 0 days). β-Actin was used as an internal control. Respective representative blot (*top*) and densitometric analysis (*bottom*) of (**A**) αV integrin, (**B**) β1 integrin, (**C**) β3 integrin, (**D**) β5 integrin, (**E**) integrin linked kinase, (**F**) focal adhesion kinase, (**G**) phospho-focal adhesion kinase. *Columns and error bars*; means and standard error of mean (SEM). Two-way ANOVA with the Holm Sidak pairwise comparisons post hoc test was used for statistical analysis ($n = 5$ biological replicates). $^{*}P < 0.05$, $^{**}P < 0.01$, $^{***}P < 0.001$ for GIM versus VehM, given significant treatment and time interaction. $^{\dagger}P < 0.05$, $^{\dagger\dagger}P < 0.01$ for GIM versus baseline protein, given significant main effect of treatment. $^{\#}P < 0.05$, $^{\#\#}P < 0.01$ for VehM versus baseline protein. VehM, vehicle control matrix; GIM, glucocorticoid-induced matrix; hTM, human trabecular meshwork.

Investigative Ophthalmology & Visual Science

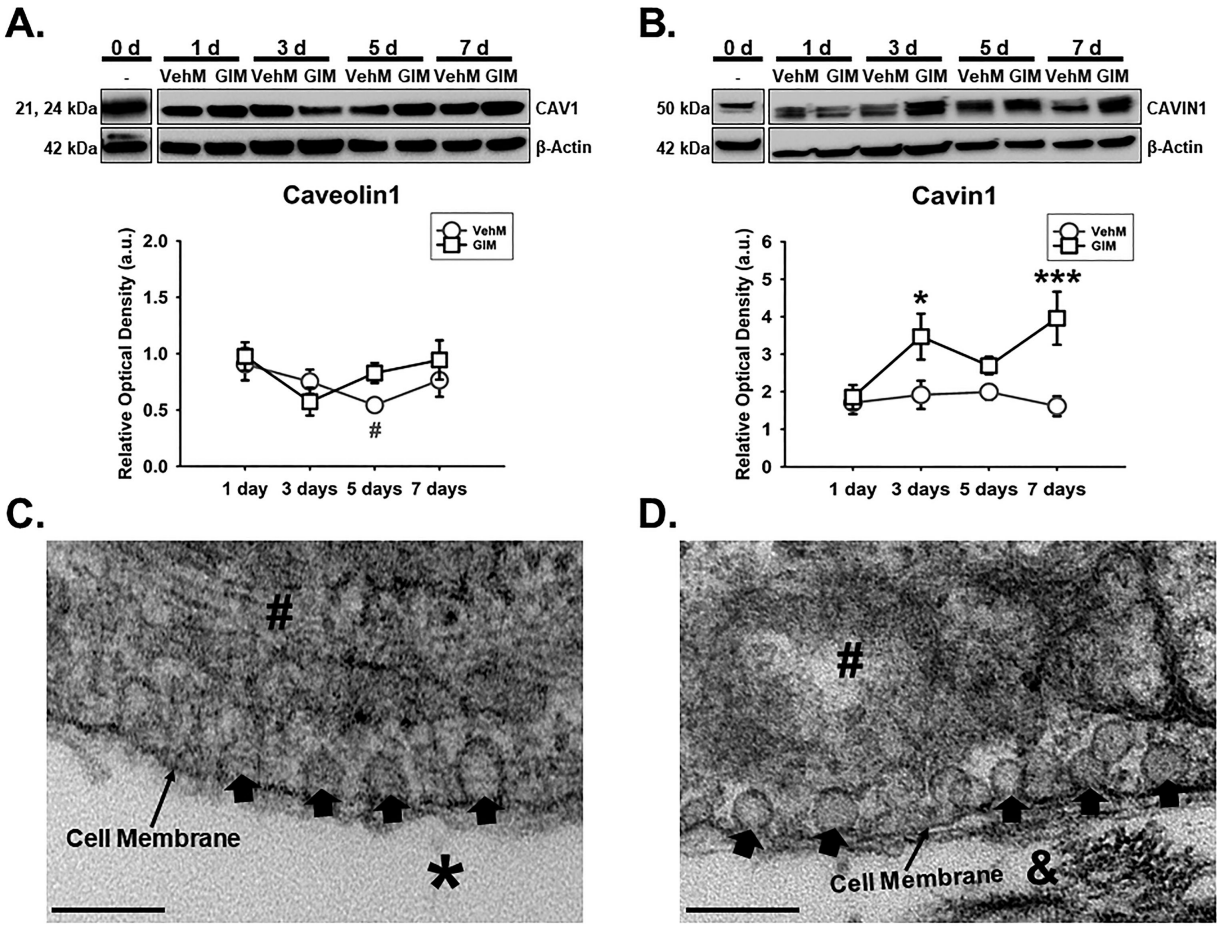

Figure 7. VehMs and GIMs form caveolae with GIMs temporally overexpressing Cavin1 in hTM cells. Primary hTM cells were treated with vehicle control (Veh) or 100 nM dexamethasone (DEX) in complete growth media for 4 weeks to obtain VehMs and GIMs, respectively, following successful decellularization. Fresh, earlier passage, hTM cells from the same donor used to obtain these matrices were cultured on VehMs and GIMs in 1% fetal bovine serum (FBS) growth media for 1, 3, 5, and 7 day(s). Protein was extracted for Western blot analysis, and transmission electron microscopy was performed to visualize caveolae. Data from VehM and GIM were respectively normalized to baseline protein levels (time point 0 day). β-Actin was used as an internal control. Respective representative blot (*top*) and densitometric analysis (*bottom*) of (**A**) Caveolin1, and (**B**) Cavin1. Representative electron micrograph demonstrating cell membrane-bound caveolae in cells cultured on (**C**) VehMs and (**D**) GIMs for 7 days. *Columns and error bars*; means and standard error of mean (SEM). Two-way ANOVA with the Holm Sidak pairwise comparisons post hoc test was used for statistical analysis ($n = 5$ biological replicates). *$P < 0.05$, ***$P < 0.001$ for GIM versus VehM, given significant treatment and time interaction. #$P < 0.05$ VehM versus baseline protein. hTM, human trabecular meshwork; VehMs, vehicle control matrices; GIMs, glucocorticoid-induced matrices. *Arrow heads*, Caveolae; #, Cytoplasm; *, VehM; &, GIM. Scale bar, 200 nm.

GIM Stiffened hTM Cells at all Time Points

Finally, a key facet of DEX-induced ocular hypertensive phenotypes is increased tissue stiffness,[7] which is associated with ocular hypertension and glaucoma.[6,43,81] Although GIM or pathological matrices can stiffen hTM cells at a single time point,[80,81] whether this GIM-induced cell stiffening is dependent on time and / or sustained across multiple time points was unknown. We thus determined the stiffness of hTM cells cultured on VehMs and GIMs for 1, 3, 5, and 7 day(s). We discovered that VehM- or GIM-induced cell stiffness was time-independent. However, whereas no marked main effect of time was observed ($F[3, 16] = 2.278$, $P = 0.1187$), there was significant main effect of treatment on cell stiffening ($F[1, 16] = 18.48$, $P = 0.0006$). Post hoc analysis showed that, compared with VehM, GIM markedly upregulated the elastic moduli of hTM cells ($P < 0.01$, $P < 0.001$, $P < 0.05$, and $P < 0.001$, respectively) at all time points (Fig. 9).

Discussion

Maintenance of aqueous homeostasis within acceptable narrow limits in response to fluctuations in intraocular pressure (IOP) is an active dynamic process, and intricately involves constant physiological remodeling of TM cells and their ECM.[21–23,74,75] Thus, in aberrant cell and/or ECM remodeling implicated in loss of aqueous homeostasis,[74,80,81] the underlying molecules/mechanisms are likely going to be changing constantly.[99–101] Very few reports on the mechanistic underpinnings of aberrant TM cell and / or ECM remodeling in fibrotic phenotypes have factored in time course experiments and / or statistically considered interaction between treatment and time. Therefore, in this study, we determined the time-dependent effects of DEX and GIM on the protein expression of specific integrin subunits, integrin adhesomes, caveolins, cytoskeletal-related proteins, and/or stiffness, concurrently in hTM cells. Whereas DEX-induced fibrotic trait in hTM cells appeared to be dependent on

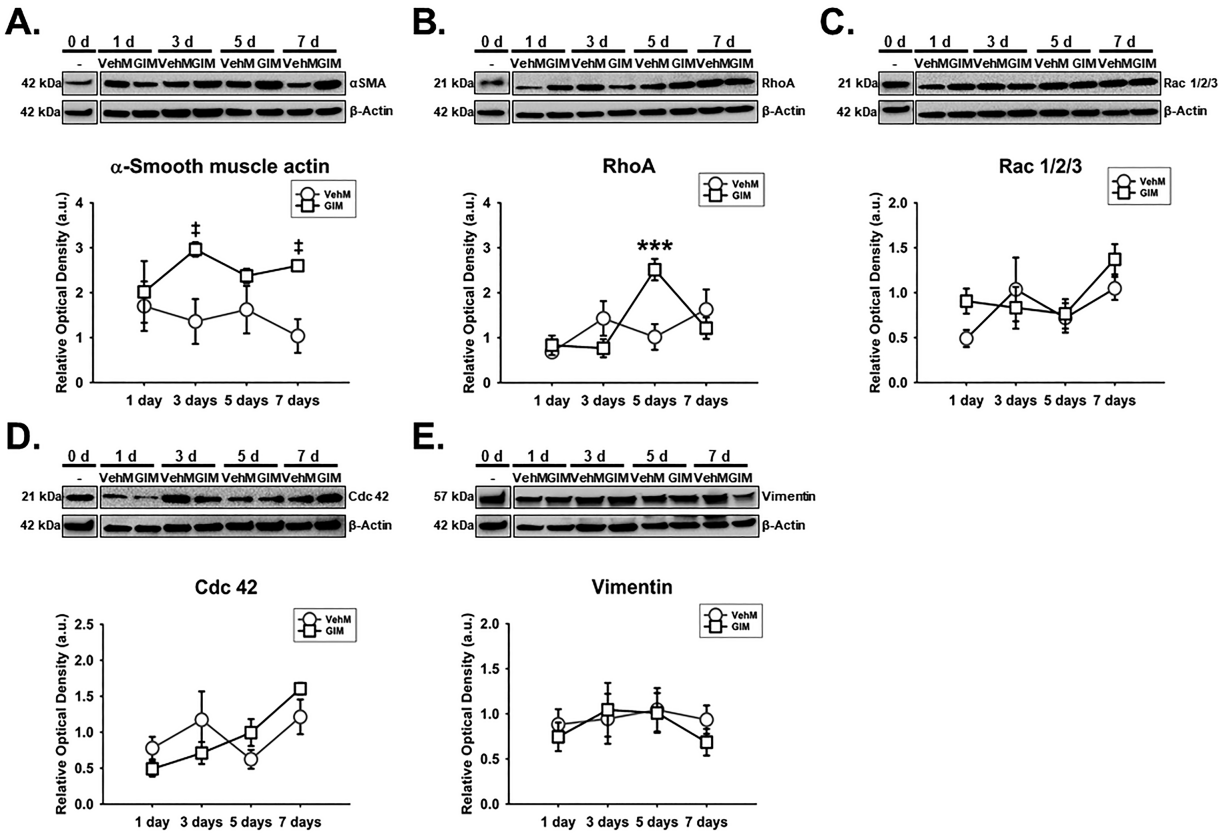

Figure 8. GIM temporally and differentially upregulated specific actin cytoskeletal-related proteins hTM cells. Primary hTM cells were cultured in the absence or presence of 100 nM dexamethasone (DEX) in complete growth media for 4 weeks and decellularized to obtain VehMs and GIMs respectively. New hTM cells from the same donor used to derive these matrices were cultured on VehMs and GIMs in 1% fetal bovine serum (FBS) growth media for 1, 3, 5, and 7 day(s). Protein was extracted for Western blot analysis. VehM and GIM were, respectively, normalized to baseline protein levels (time point 0 day). β-Actin was used as an internal control. Respective representative blot (*top*) and densitometric analysis (*bottom*) of (**A**) α-smooth muscle actin, (**B**) RhoA, (**C**) Rac 1/2/3, (**D**) Cdc 42, (**E**) vimentin. *Columns and error bars*; means and standard error of mean (SEM). Two-way ANOVA with the Holm Sidak pairwise comparisons post hoc test was used for statistical analysis ($n = 5$ biological replicates). $^{***}P < 0.001$ for GIM versus VehM, given significant treatment and time interaction. $^{‡}P < 0.05$ for GIM versus VehM, given significant main effect of treatment). hTM, human trabecular meshwork; VehM, vehicle control matrix; GIM, glucocorticoid-induced matrix.

activation of the glucocorticoid receptor (by time-dependent overexpression of one of its primary response proteins, FK506 binding protein 5 [Supplementary Fig. S1A]), that of GIM might have primarily been driven by ECM-derived factors including FN ED-A and FN ED-B, which have been implicated in ocular hypertension and/or POAG,[40,95,96] and most likely independent of direct influences from the glucocorticoid receptor (Supplementary Fig. S1B). Although the increase in immunostaining demonstrated for FN ED-A and FN ED-B in GIMs is qualitative in the current study, quantitative tools in confocal microscopy in addition to multiple redundant approaches may be essential to definitively document the precise relative quantities of these isoforms in future investigation.[102,103]

DEX and GIM Temporally and Differentially Sustain Elevation of Key Integrin Subunits, Integrin Adhesomes, and / or Caveolins in hTM Cells

First, we observed that exogenous DEX not only sustained upregulation of αV, β3, and β5 integrins, and ILK in hTM cells, but was dependent on time. DEX-induced sustained increase of these molecules at the protein level could probably be due to increases in half-lives and synthesis rates of their respective mRNAs over time.[46] Almost all these mechanoreceptors and integrin adhesome have been implicated in fibrotic phenotypes and/or ocular hypertension at least at a single time point. For example, the role of integrins in the increased formation of CLANs, fibrillogenesis of fibronectin and impaired phagocytosis have all been reported.[30,34,40,46,104] A recent study showed that reduction of β3 integrin expression alone decreased IOP in vivo in mice.[56] Further, β5 integrin has been implicated in phagocytosis, an important function of hTM cells implicated in outflow homeostasis.[34] However, there is evidence DEX impairs phagocytosis.[35] Thus, DEX-induced time-dependent sustained elevation of β5 integrin may suggest aberrant phagocytosis, which could paradoxically favor deposition of fibrotic phenotypes in hTM cells. Alternatively, regardless of the expression levels of β5 integrin, β3 integrin could probably inhibit the former's physiologic function in phagocytosis, to tip the balance toward a fibrotic phenotype in agreement with previous studies.[34]

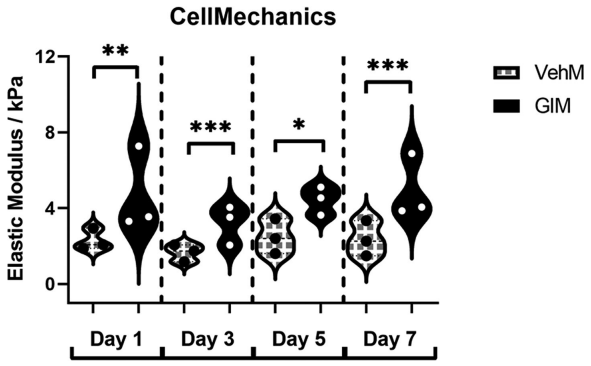

Figure 9. GIMs stiffened seeded hTM cells across all timepoints. Primary hTM cells were cultured in the presence or absence of 100 nM dexamethasone for 4 weeks in complete growth media. Cells were subsequently removed using 20 mM ammonium hydroxide solution to obtain GIMs and vehicle control matrices (VehMs). Earlier passage, fresh primary hTM cells were then seeded on these matrices in 1% fetal bovine serum growth media for 1-, 3-, 5-, and 7-day time points. Subsequently, cell mechanics was determined via atomic force microscopy. Cello plots (each data point represents elastic modulus derived from a single force curve; five of such force curves were obtained from a single random cell; total force curves were obtained from at least nine random cells per experimental group) demonstrate hTM cells cultured on GIMs were stiffer at all time points in comparison with those on VehMs. Two-way ANOVA was used to determine the main effects of treatment and time and/or their interaction for VehM versus GIM ($n = 3$ biological replicates). $^{*}P < 0.05$, $^{**}P < 0.01$, $^{***}P < 0.001$ for VehM versus GIM. hTM, human trabecular meshwork; VehM, vehicle control matrix; GIM, glucocorticoid-induced matrix.

On the other hand, GIM maintained upregulation of αV integrin and Cavin1 in a time-dependent manner in hTM cells. These molecules have also been implicated in fibrotic phenotypes. For instance, αV integrin is overexpressed by TGFβ2 and connective tissue growth factor implicated in elevated IOP and POAG.[104–106] While αV integrin has mostly been described in the context of β3 and β5 integrins, at least in the TM,[30,34,38,46] it can also dimerize with β6 or β8 integrins to bind to a number of ECM and soluble ligands, including but not limited to fibronectin, vitronectin, osteopontin, TGFβ latency associated peptide, laminin, fibrillin, tenascin, laminin, and fibrinogen.[107–110] Given that GIM had no significant impact on the expression of β1, β3, or β5 integrins, whether αV integrin associates with other integrins (for instance, β6 or β8 integrins, relatively under-reported in the TM[111]), if any, to drive and sustain GIM-induced ocular hypertensive phenotypes in hTM cells warrants further investigations.

Further, we observed DEX-mediated overexpression of Cavin1 in hTM cells was sustained on day 7, but not dependent on time. In contrast, sustained overexpression of Cavin1 by GIM was time dependent. The normal mechanosensitive function of caveolae, which is important for aqueous homeostasis and IOP regulation,[58] is predominantly dependent on dissociation of Cavin1, resulting in caveolae disassembly.[58,71,72,112] Thus, it is likely that Cavin1 overexpression results in aberrant loss of caveolae over time consistent with previous studies;[72,86] with subsequent impairment of caveolae's physiologic mechanosensitive function in hTM cells. Whereas we did not quantitate the density or distribution of caveolae in the current study, for the first time, we did observe their occurrence in hTM cells cultured on VehM and GIM. Defining the specific dynamic relationship between expression of caveolae-related proteins (for instance, Cavin1) and caveolae assembly / disassembly by VehM or GIM in hTM cells remains to be investigated; this would certainly be predicated on establishing appropriate methods to quantify caveolae and its dynamics.

DEX and GIM Temporally and Differentially Modulate Specific Cytoskeletal-Related Proteins and Cell Contractility in hTM Cells

Downstream of mechanoreceptors are their effectors, including actin-related proteins like Rho GTPases, which regulate actin cytoskeleton,[49,65,113] and intermediate filament vimentin. Here, we show that DEX transiently upregulated RhoA in hTM cells, and this transient increase was time-dependent, consistent with prior studies that reported increased cell contractility, and/or fibrotic changes in hTM cells[49,51,65] and non-ocular tissues.[50] Although there was significant interaction between treatment and time for the expression of Rac 1/2/3 in hTM cells, no marked differences were observed between Veh and DEX. This finding may probably suggest DEX-induced fibrotic phenotypes in hTM cells is independent of Rac 1,[33] which may be dormant in hTM cells.

Further, DEX sustained the downregulation of Cdc42 in a time-dependent manner in hTM cells. Cdc42 has been implicated in cell-cell communication (via formation of tunneling nanotubes)[114] important for aqueous homeostasis.[115] Therefore, DEX-induced temporal reduction of Cdc42 in hTM cells could probably indicate their dynamic homeostatic function in cell-cell communication is compromised. Concurrently, DEX sustained the upregulation of αSMA in hTM cells in a time-dependent manner, indicating increased cell contractility over time in glaucoma.[28]

On the other hand, for the first time, we demonstrate GIM transiently elevated RhoA in hTM cells in a time-dependent manner. The other Rho GTPases were not significantly impacted by GIM. The differential modulation of these Rho GTPases by DEX and GIM may be due to their ligand- and context-dependent nature. For example, migration of rat glioblastoma cells in brain parenchyma showed higher Rac 1 and Cdc42, and lower RhoA activities, than migration in the perivascular regions.[116] Finally, GIM (in the absence of DEX) sustained the upregulation of αSMA in hTM cells independent of time, indicating increased cell contractility implicated in glaucoma[28] may prevail irrespective of time.

Veh and VehM Temporally and Differentially Modulate Expression of Specific Mechanosensitive Molecules in hTM Cells

Under normal circumstances, vehicle controls are not expected to have significant impacts on experimental outcomes compared with normal baseline controls. However, surprisingly, in this study, compared with baseline proteins, Veh (that is, vehicle control for DEX) and VehM (that is, vehicle control for GIM) differentially modulated specific integrin subunits, integrin adhesomes, caveolins, and cytoskeletal-related proteins in a time-dependent or independent manner. For instance, Veh did have a small but significant permanent reduction in the protein expression of β3 integrin in a time-dependent manner compared with baseline protein levels. This agrees with previous

studies that showed Veh can diminish the protein levels of β3 integrin[46] and other genes[33] at multiple time points. This trend was not exclusive to β3 integrin; the same was observed for β1 integrin, ILK, FAK, Cavin1, α-SMA, RhoA, Rac 1/2/3, and vimentin; transient or sustained increase/decrease, with or without time interaction. It is feasible these unexpected changes may indicate critical thresholds beyond or below which the probable physiologic functions of respective molecules may become pathologic. Similarly, although less prevalent, VehM transiently impacted the expression of molecules like αV and β1 integrins, and Caveolin1 compared with baseline proteins. Whereas this observation might have negatively or positively affected the impact of DEX (for instance, β1 integrin) and GIM on these molecules, it could probably be dependent on (1) intrinsic variations in baseline protein levels of donor tissues (using β3 integrin as a representative; Supplementary Fig. S2), (2) differences in the protein of interest (for instance, αV integrin versus β3 integrin), (3) differences in the specific ligand / stimulant involved (for example, Veh versus VehM), (4) differences in time-dependent changes regardless of treatment, and / or (5) differences in donors' initial response to DEX.[117]

GIM Sustain Stiffening of hTM Cells Across all Time Points

We recently documented crosslinked CDM stiffens hTM cells[81] and our group has previously reported DEX increases stiffness of hTM cells[7]; herein, we document that GIM-mediated increased cell stiffening is consistent across multiple time points. Several studies have implicated substratum stiffness,[118] integrins,[73] caveolins,[119] and Rho GTPases[50,120–122] in altered biomechanics in ocular and non-ocular cells / tissues. Therefore, the time-independent increase in stiffness of cells cultured on GIMs may be due in part to the integration of FN ED-A / FN ED-B overexpression, specific integrins, caveolins and Rho GTPases in hTM cells or aberrant TGFβ2 signaling.[68]

Limitations

We recognize that this study is not without limitations. First, because our furthest time point was 7 days, we conducted all our experiments in 1% serum growth media. This was to ensure cell survival, while minimizing the effects of serum proteins as a confounding factor in our experimental outcomes. However, it is feasible that growth factors and cytokines present even in a small percentage of serum may have an impact on the various end points in our study. While serum-free conditions may appear to better minimize such an effect, one may still have to contend with cells becoming stressed over time as a confounder. This is especially important considering substratum properties can dictate cellular responses to stress. In addition, our optimized chronic approaches for generating CDMs (for instance, VehMs and GIMs)[77] almost always result in relatively dense and robust matrices that firmly adhere to their plastic / glass substrates. However, there could be variations in the amount of ECM deposited due to the natural variation among donors, variations in responses to stimulants, and time-dependent differences in ECM remodeling. Quantifying the protein levels of deposited ECM from donors and over time for normalization purposes might have reduced probable variations in VehM- or GIM-induced cellular changes in the current study. Finally, whereas we report changes in the protein expression of certain cytoskeletal proteins of the Rho GTPase family, determining their activity or phosphorylated states in the current study would have enhanced understanding of their definitive roles in cellular homeostasis or fibrotic phenotypes.

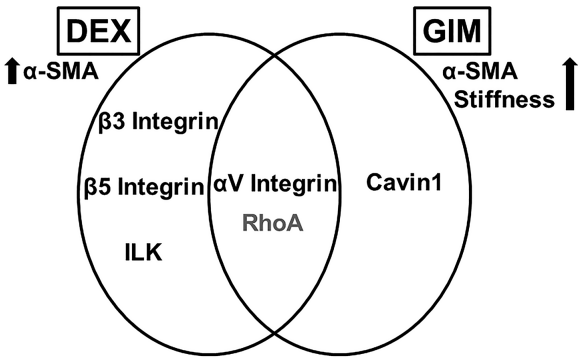

Figure 10. Venn diagram summarizing molecules whose time-dependent overexpression may sustain DEX- or GIM-induced fibrotic phenotypes. ILK, integrin linked kinase; α-SMA, α-smooth muscle actin. *Black font color*, permanently overexpressed. *Gray font color*, transiently overexpressed.

Conclusion

In conclusion, to the best of our knowledge, this is the first report on the time-dependent or independent interaction with DEX or a pathologically remodeled ECM (that is, GIM) on the protein expression of a wide range of molecules spanning from specific mechanoreceptors (that is, integrin subunits, integrin adhesomes, and caveolins) to key cytoskeletal-related proteins (that is, Rho GTPases and vimentin); associated with ocular hypertensive phenotypes (for example, increased cell contractility and/or stiffness) in hTM cells. Whereas some of these molecules may underpin DEX- or GIM-induced fibrotic phenotypes in hTM cells over time (Fig. 10), whether normal hTM cells can in turn modify GIMs over time either as an adaptive response or perpetuation toward pathologic phenotype remains to be seen.

Acknowledgments

The authors thank Margaret Gondo for technical assistance, and Opoku-Baah Collins for assistance with programming in Matlab for data analysis, and their funding sources: Bright Focus National Glaucoma Research Award (V.K.R.), startup funding at University of Houston College of Optometry (UHCO; V.K.R.), student Vision Research Support Grant at UHCO (F.Y.), and National Institute of Health grants 1R01EY026048 (V.K.R.), and 5P30EY007551. Finally, we would like to thank the organ donors and SavingSight eye bank for the donor tissues used in this study.

Supported by Bright Focus National Glaucoma Research Award (V.K.R.), startup funding at University of Houston College of Optometry (UHCO; V.K.R.), student Vision Research Support Grant at UHCO (F.Y.), and National Institute of Health grants 1R01EY026048 (V.K.R.), and 5P30EY007551.

Disclosure: **F. Yemanyi,** None; **H. Baidouri,** None; **A.R. Baidouri,** None; **V. Raghunathan,** None

References

1. Rozsíval P, Hampl R, Obenberger J, Stárka L, Řehák S. Aqueous humour and plasma cortisol levels in glaucoma and cataract patients. *Curr Eye Res*. 1981;1(7):391–396.
2. Southren AL, Gordon GG, Munnangi PR, et al. Altered cortisol metabolism in cells cultured from trabecular meshwork specimens obtained from patients with primary open-angle glaucoma. *Invest Ophthalmol Vis Sci*. 1983;24(10):1413–1417.
3. Weinstein BI, Munnangi P, Gordon GG, Southren AL. Defects in cortisol-metabolizing enzymes in primary open-angle glaucoma. *Invest Ophthalmol Vis Sci*. 1985;26(6):890–893.
4. Clark AF, Wordinger RJ. The role of steroids in outflow resistance. *Exp Eye Res*. 2009;88(4):752–759.
5. Bollinger KE, Crabb JS, Yuan X, Putliwala T, Clark AF. Proteomic similarities in steroid responsiveness in normal and glaucomatous trabecular meshwork cells. *Mol Vis*. 2012;18:2001–2011.
6. Last JA, Pan T, Ding Y, et al. Elastic modulus determination of normal and glaucomatous human trabecular meshwork. *Investig Ophthalmol Vis Sci*. 2011;52(5):2147–2152.
7. Raghunathan VK, Morgan JT, Park SA, et al. Dexamethasone stiffens trabecular meshwork, trabecular meshwork cells, and matrix. *Investig Ophthalmol Vis Sci*. 2015;56(8):4447–4459.
8. Grant WM. Experimental aqueous perfusion in enucleated human eyes. *Arch Ophthalmol*. 1963;69(6):783–801.
9. Tektas OY, Lütjen-Drecoll E. Structural changes of the trabecular meshwork in different kinds of glaucoma. *Exp Eye Res*. 2009;88(4):769–775.
10. Ramamoorthy S, Cidlowski JA. Corticosteroids: mechanisms of action in health and disease. *Rheum Dis Clin North Am*. 2016;42(1):15–31.
11. Patel GC, Millar JC, Clark AF. Glucocorticoid receptor transactivation is required for glucocorticoid-induced ocular hypertension and glaucoma. *Investig Ophthalmol Vis Sci*. 2019;60(6):1967–1978.
12. Fini ME, Schwartz SG, Gao X, et al. Steroid-induced ocular hypertension/glaucoma: Focus on pharmacogenomics and implications for precision medicine. *Prog Retin Eye Res*. 2017;56:58–83.
13. Rhen T, Cidlowski JA. Antiinflammatory action of glucocorticoids - new mechanisms for old drugs. *N Engl J Med*. 2005;353(16):1711–1723.
14. Becker B, Mills DW. Corticosteroids and intraocular pressure. *Arch Ophthalmol*. 1963;70(4):500–507.
15. Armaly M. Effect of corticosteroids fluid dynamics. *Arch Ophthalmol*. 1963;70(4):482–491.
16. Dibas A, Yorio T. Glucocorticoid therapy and ocular hypertension. *Eur J Pharmacol*. 2016;787:57–71.
17. Kersey JP, Broadway DC. Corticosteroid-induced glaucoma: a review of the literature. *Eye*. 2006;20(4):407–416.
18. Bernstein HN, Mills DW, Becker B. Steroid-induced elevation of intraocular pressure. *Arch Ophthalmol*. 1963;70(1):15–18.
19. Jones R, Rhee DJ. Corticosteroid-induced ocular hypertension and glaucoma: a brief review and update of the literature. *Curr Opin Ophthalmol*. 2006;17(2):163–167.
20. Wilson K, McCartney MD, Miggans ST, Clark AF. Dexamethasone induced ultrastructural changes in cultured human trabecular meshwork cells. *Curr Eye Res*. 1993;12(9):783–793.
21. Acott TS, Kelley MJ. Extracellular matrix in the trabecular meshwork. *Exp Eye Res*. 2008;86(4):543–561.
22. Stamer WD, Acott TS. Current understanding of conventional outflow dysfunction in glaucoma. *Curr Opin Ophthalmol*. 2012;23(2):135–143.
23. Vranka JA, Kelley MJ, Acott TS, Keller KE. Extracellular matrix in the trabecular meshwork: intraocular pressure regulation and dysregulation in glaucoma. *Exp Eye Res*. 2015;133:112–125.
24. Rohen J, Lutjen-Drecoll E, Flugel C, Meyer M, Grierson I. Ultrastructure of the trabecular meshwork in untreated cases of POAG.pdf. *Exp Eye Res*. 1993;56:683–692.
25. Clark AF, Wilson K, de Kater AW, Allingham RR, McCartney MD. Dexamethasone-induced ocular hypertension in perfusion-cultured human eyes. *Invest Ophthalmol Vis Sci*. 1995;36(2):478–489.
26. Kasetti RB, Maddineni P, Patel PD, Searby C, Sheffield VC, Zode GS. Transforming growth factor $\beta 2$ (TGF$\beta 2$) signaling plays a key role in glucocorticoid-induced ocular hypertension. *J Biol Chem*. 2018;293(25):9854–9868.
27. Zode GS, Sharma AB, Lin X, et al. Ocular-specific ER stress reduction rescues glaucoma in murine glucocorticoid-induced glaucoma. *J Clin Invest*. 2014;124(5):1956–1965.
28. Clark AF, Brotchie D, Read AT, et al. Dexamethasone alters F-actin architecture and promotes cross-linked actin network formation in human trabecular meshwork tissue. *Cell Motil Cytoskeleton*. 2005;60(2):83–95.
29. Clark AF, Wilson K, McCartney MD, Miggans ST, Kunkle M, Howe W. Glucocorticoid-induced formation of cross-linked actin networks in cultured human trabecular meshwork cells. *Invest Ophthalmol Vis Sci*. 1994;35(1):281–294.
30. Filla MS, Schwinn MK, Nosie AK, Clark RW, Peters DM. Dexamethasone-associated cross-linked actin network formation in human trabecular meshwork cells involves $\beta 3$ integrin signaling. *Investig Ophthalmol Vis Sci*. 2011;52(6):2952–2959.
31. Clark AF, Lane D, Wilson K, Miggans ST, McCartney MD. Inhibition of dexamethasone-induced cytoskeletal changes in cultured human trabecular meshwork cells by tetrahydrocortisol. *Investig Ophthalmol Vis Sci*. 1996;37(5):805–813.
32. Clark R, Nosie A, Walker T, et al. Comparative genomic and proteomic analysis of cytoskeletal changes in dexamethasone-treated trabecular meshwork cells. *Mol Cell Proteomics*. 2013;12(1):194–206.
33. Faralli JA, Desikan H, Peotter J, et al. Genopic/proteomic analyses of dexamethasone-treated human trabecular meshwork cells reveal a role for GULP1 and ABR in phagocytosis. *Mol Vis*. 2019;25:237–254.
34. Gagen D, Filla MS, Clark R, Liton P, Peters DM. Activated $\alpha v\beta 3$ integrin regulates $\alpha v\beta 5$ integrin-mediated phagocytosis in trabecular meshwork cells. *Investig Ophthalmol Vis Sci*. 2013;54(7):5000–5011.
35. Matsumoto Y, Johnson DH. Dexamethasone decreases phagocytosis by human trabecular meshwork cells in situ. *Investig Ophthalmol Vis Sci*. 1997;38(9):1902–1907.
36. Kasetti RB, Maddineni P, Millar JC, Clark AF, Zode GS. Increased synthesis and deposition of extracellular matrix proteins leads to endoplasmic reticulum stress in the trabecular meshwork. *Sci Rep*. 2017;7(1):14951.
37. Steely HT, Browder SL, Julian MB, Miggans ST, Wilson KL, Clark AF. The effects of dexamethasone on fibronectin expression in cultured human trabecular meshwork cells. *Investig Ophthalmol Vis Sci*. 1992;33(7):2242–2250.
38. Dickerson J, Steely H, English-Wright S, Clark A. The effect of dexamethasone on integrin and laminin expression in cultured human trabecular meshwork cells. *Exp Eye Res*. 1998;66:731–738.

39. Faralli JA, Schwinn MK, Gonzalez JM, Filla MS, Peters DM. Functional properties of fibronectin in the trabecular meshwork. *Exp Eye Res*. 2009;88(4):689–693.
40. Filla MS, Faralli JA, Desikan H, Peotter JL, Wannow AC, Peters DM. Activation of $\alpha v\beta 3$ integrin alters fibronectin fibril formation in human trabecular meshwork cells in a ROCK-independent manner. *Investig Ophthalmol Vis Sci*. 2019;60(12):3897–3913.
41. Zhou L, Li Y, Yue BY. Glucocorticoid effects on extracellular matrix proteins and integrins in bovine trabecular meshwork cells in relation to glaucoma. *Int J Mol Med*. 1998;1(2):339–346.
42. Flügel-Koch C, Ohlmann A, Fuchshofer R, Welge-Lüssen U, Tamm ER. Thrombospondin-1 in the trabecular meshwork: localization in normal and glaucomatous eyes, and induction by TGF-β1 and dexamethasone in vitro. *Exp Eye Res*. 2004;79(5):649–663.
43. Wang K, Li G, Read AT, et al. The relationship between outflow resistance and trabecular meshwork stiffness in mice. *Sci Rep*. 2018;8(1):5848.
44. Faralli JA, Newman JR, Sheibani N, Dedhar S, Peters DM. Integrin-linked kinase regulates integrin signaling in human trabecular meshwork cells. *Investig Ophthalmol Vis Sci*. 2011;52(3):1684–1692.
45. Filla MS, Faralli JA, Peotter JL, Peters DM. The role of integrins in glaucoma. *Exp Eye Res*. 2017;158:124–136.
46. Faralli JA, Gagen D, Filla MS, Crotti TN, Peters DM. Dexamethasone increases $\alpha v\beta 3$ integrin expression and affinity through a calcineurin/NFAT pathway. *Biochim Biophys Acta - Mol Cell Res*. 2013;1833(12):3306–3313.
47. Surgucheva I, Surguchov A. Expression of caveolin in trabecular meshwork cells and its possible implication in pathogenesis of primary open angle glaucoma. *Mol Vis*. 2011;17:2878–2888.
48. Qiu X, Wu K, Lin X, Liu Q, Ye Y, Yu M. Dexamethasone increases Cdc42 expression in human TM-1 cells. *Curr Eye Res*. 2015;40(3):290–299.
49. Pattabiraman PP, Rao PV. Mechanistic basis of Rho GTPase-induced extracellular matrix synthesis in trabecular meshwork cells. *Am J Physiol - Cell Physiol*. 2009;298(3):749–763.
50. Kunschmann T, Puder S, Fischer T, Steffen A, Rottner K, Mierke CT. The small GTPase Rac1 increases cell surface stiffness and enhances 3D migration into extracellular matrices. *Sci Rep*. 2019;9(1):7675.
51. Pattabiraman PP, Inoue T, Rao PV. Elevated intraocular pressure induces Rho GTPase mediated contractile signaling in the trabecular meshwork. *Exp Eye Res*. 2015;136:29–33.
52. Ashok A, Kang MH, Wise AS, et al. Prion protein modulates endothelial to mesenchyme-like transition in trabecular meshwork cells: Implications for primary open angle glaucoma. *Sci Rep*. 2019;9(1):13090.
53. Morgan JT, Raghunathan VK, Chang YR, Murphy CJ, Russell P. The intrinsic stiffness of human trabecular meshwork cells increases with senescence. *Oncotarget*. 2015;6(17):15362–15374.
54. Filla MS, Woods A, Kaufman PL, Peters DM. B1 and B3 integrins cooperate to induce syndecan-4-containing cross-linked actin networks in human trabecular meshwork cells. *Investig Ophthalmol Vis Sci*. 2006;47(5):1956–1967.
55. Filla MS, Schwinn MK, Sheibani N, Kaufman PL, Peters DM. Regulation of cross-linked actin network (CLAN) formation in human trabecular meshwork (HTM) cells by convergence of distinct β1 and β3 integrin pathways. *Investig Ophthalmol Vis Sci*. 2009;50(12):5723–5731.
56. Faralli JA, Filla MS, Peters DM. Effect of alphaVbeta3 integrin expression and activity on intraocular pressure. *Investig Ophthalmol Vis Sci*. 2019;60:1776–1788.
57. Aga M, Bradley JM, Wanchu R, Yang YF, Acott TS, Keller KE. Differential effects of caveolin-1 and -2 knockdown on aqueous outflow and altered extracellular matrix turnover in caveolin-silenced trabecular meshwork cells. *Investig Ophthalmol Vis Sci*. 2014;55(9):5497–5509.
58. Elliott MH, Ashpole NE, Gu X, et al. Caveolin-1 modulates intraocular pressure: implications for caveolae mechanoprotection in glaucoma. *Sci Rep*. 2016;6:37127.
59. Wu Z, Huang C, Xu C, et al. Caveolin-1 regulates human trabecular meshwork cell adhesion, endocytosis, and autophagy. *J Cell Biochem*. 2019;120(8):13382–13391.
60. Liu CY, Lin HH, Tang MJ, Wang YK. Vimentin contributes to epithelial-mesenchymal transition cancer cell mechanics by mediating cytoskeletal organization and focal adhesion maturation. *Oncotarget*. 2015;6(18):15966–15983.
61. Collins C, Guilluy C, Welch C, et al. Localized tensional forces on PECAM-1 elicit a global mechanotransduction response via the integrin-RhoA pathway. *Curr Biol*. 2012;22(22):2087–2094.
62. Moreno-Vicente R, Pavón DM, Martín-Padura I, et al. Caveolin-1 modulates mechanotransduction responses to substrate stiffness through actin-dependent control of YAP. *Cell Rep*. 2018;25(6):1622–1635.
63. Joshi B, Strugnell SS, Goetz JG, et al. Phosphorylated caveolin-1 regulates Rho/ROCK-dependent focal adhesion dynamics and tumor cell migration and invasion. *Cancer Res*. 2008;68(20):8210–8220.
64. Sharma S, Santiskulvong C, Rao J, Gimzewski JK, Dorigo O. The role of Rho GTPase in cell stiffness and cisplatin resistance in ovarian cancer cells. *Integr Biol (United Kingdom)*. 2014;6(6):611–617.
65. Rao PV, Pattabiraman PP, Kopczynski C. Role of the Rho GTPase/Rho kinase signaling pathway in pathogenesis and treatment of glaucoma: bench to bedside research. *Exp Eye Res*. 2017;158:23–32.
66. Espildora J, Vicuna P, Diaz E. [Cortisone-induced glaucoma: a report on 44 affected eyes (author's translation)]. *J Fr Ophtalmol*. 1981;4(6–7):503–508.
67. François J. Corticosteroid glaucoma. *Ann Ophthalmol*. 1977;9(9):1075–1080.
68. Yemanyi F, Vranka J, Raghunathan VK. Glucocorticoid-induced cell-derived matrix modulates transforming growth factor β2 signaling in human trabecular meshwork cells. *Sci Rep*. 2020;10(1):15641.
69. Du J, Zu Y, Li J, et al. Extracellular matrix stiffness dictates Wnt expression through integrin pathway. *Sci Rep*. 2016;6(February):20395.
70. Yeh YC, Ling JY, Chen WC, Lin HH, Tang MJ. Mechanotransduction of matrix stiffness in regulation of focal adhesion size and number: reciprocal regulation of caveolin-1 and β1 integrin. *Sci Rep*. 2017;7(1):15008.
71. Parton RG, Del Pozo MA. Caveolae as plasma membrane sensors, protectors and organizers. *Nat Rev Mol Cell Biol*. 2013;14(2):98–112.
72. Sinha B, Köster D, Ruez R, et al. Cells respond to mechanical stress by rapid disassembly of caveolae. *Cell*. 2011;144(3):402–413.
73. Kechagia JZ, Ivaska J, Roca-Cusachs P. Integrins as biomechanical sensors of the microenvironment. *Nat Rev Mol Cell Biol*. 2019;20(8):457–473.
74. Vranka JA, Staverosky JA, Reddy AP, et al. Biomechanical rigidity and quantitative proteomics analysis of segmental regions of the trabecular meshwork at physiologic and elevated pressures. *Investig Ophthalmol Vis Sci*. 2018;59(1):246–259.

Investigative Ophthalmology & Visual Science

75. Acott TS, Kelley MJ, Keller KE, et al. Intraocular pressure homeostasis: maintaining balance in a high-pressure environment. *J Ocul Pharmacol Ther*. 2014;30(2–3):94–101.
76. Keller KE, Bhattacharya SK, Borrás T, et al. Consensus recommendations for trabecular meshwork cell isolation, characterization and culture. *Exp Eye Res*. 2018;171:164–173.
77. Yemanyi F, Vranka J, Raghunathan VK. Generating cell-derived matrices from human trabecular meshwork cell cultures for mechanistic studies. *Methods Cell Biol*. 2020;156:271–307.
78. Raghunathan VK, Morgan JT, Chang YR, et al. Transforming growth factor beta 3 modifies mechanics and composition of extracellular matrix deposited by human trabecular meshwork cells. *ACS Biomater Sci Eng*. 2015;1(2):110–118.
79. Kaukonen R, Jacquemet G, Hamidi H, Ivaska J. Cell-derived matrices for studying cell proliferation and directional migration in a complex 3D microenvironment. *Nat Protoc*. 2017;12(11):2376–2390.
80. Raghunathan VK, Benoit J, Kasetti R, et al. Glaucomatous cell derived matrices differentially modulate non-glaucomatous trabecular meshwork cellular behavior. *Acta Biomater*. 2018;71:444–459.
81. Yemanyi F, Vranka J, Raghunathan VK. Crosslinked extracellular matrix stiffens human trabecular meshwork cells via dysregulating β-catenin and YAP/TAZ signaling pathways. *Investig Opthalmology Vis Sci*. 2020;61(10):41.
82. Chang YR, Raghunathan VK, Garland SP, Morgan JT, Russell P, Murphy CJ. Automated AFM force curve analysis for determining elastic modulus of biomaterials and biological samples. *J Mech Behav Biomed Mater*. 2014;37:209–218.
83. Gagen D, Faralli JA, Filla MS, Peters DM. The role of integrins in the trabecular meshwork. *J Ocul Pharmacol Ther*. 2014;30(2-3):110–120.
84. Humphries JD, Chastney MR, Askari JA, Humphries MJ. Signal transduction via integrin adhesion complexes. *Curr Opin Cell Biol*. 2019;56:14–21.
85. Horton ER, Astudillo P, Humphries MJ, Humphries JD. Mechanosensitivity of integrin adhesion complexes: role of the consensus adhesome. *Exp Cell Res*. 2016;343(1):7–13.
86. Rausch V, Bostrom JR, Park J, et al. The Hippo pathway regulates caveolae expression and mediates flow response via caveolae. *Curr Biol*. 2019;29(2):242–255.
87. Parton RG, Simons K. The multiple faces of caveolae. *Nat Rev Mol Cell Biol*. 2007;8(3):185–194.
88. Raghunathan VK, Morgan JT, Dreier B, et al. Role of substratum stiffness in modulating genes associated with extracellular matrix and mechanotransducers YAP and TAZ. *Investig Ophthalmol Vis Sci*. 2013;54(1):378–386.
89. Han H, Wecker T, Grehn F. Elasticity-dependent modulation of TGF-ß responses in human trabecular meshwork cells. *Investig Opthalmology Vis Sci*. 2011;52(6):2889–2896.
90. Schlunck G, Han H, Wecker T, Kampik D, Meyer-ter-Vehn T, Grehn F. Substrate rigidity modulates cell-matrix interactions and protein expression in human trabecular meshwork cells. *Investig Ophthalmol Vis Sci*. 2008;49(1):262–269.
91. Wood JA, McKee CT, Thomasy SM, et al. Substratum compliance regulates human trabecular meshwork cell behaviors and response to latrunculin B. *Investig Ophthalmol Vis Sci*. 2011;52(13):9298–9303.
92. Dupont S, Morsut L, Aragona M, et al. Role of YAP/TAZ in mechanotransduction. *Nature*. 2011;474(7350):179–184.
93. Pelham RJ, Wang YL. Cell locomotion and focal adhesions are regulated by substrate flexibility. *Proc Natl Acad Sci U S A*. 1997;94(25):13661–13665.
94. Yemanyi F, Vranka JA, Raghunathan V. Crosslinked ECM modulates β-Catenin and YAP/TAZ pathways in human trabecular meshwork cells. *Invest Ophthalmol Vis Sci*. 2020;61(7):1434.
95. Medina-Ortiz WE, Belmares R, Neubauer S, Wordinger RJ, Clark AF. Cellular fibronectin expression in human trabecular meshwork and induction by transforming growth factor-β2. *Investig Ophthalmol Vis Sci*. 2013;54(10):6779–6788.
96. Filla MS, Dimeo KD, Tong T, Peters DM. Disruption of fibronectin matrix affects type IV collagen, fibrillin and laminin deposition into extracellular matrix of human trabecular meshwork (HTM) cells. *Exp Eye Res*. 2017;165:7–19.
97. Roberts AL, Mavlyutov TA, Perlmutter TE, et al. Fibronectin extra domain A (FN-EDA) elevates intraocular pressure through toll-like receptor 4 signaling. *Sci Rep*. 2020;10(1):9815.
98. Hernandez H, Roberts AL, McDowell CM. Nuclear factor-kappa beta signaling is required for transforming growth factor Beta-2 induced ocular hypertension. *Exp Eye Res*. 2020;191.
99. Vranka JA, Acott TS. Pressure-induced expression changes in segmental flow regions of the human trabecular meshwork. *Exp Eye Res*. 2017;158:67–72.
100. Vranka JA, Staverosky JA, Raghunathan VK, Acott TS. Elevated pressure influences relative distribution of segmental regions of the trabecular meshwork. *Exp Eye Res*. 2020;190:107888.
101. Vranka JA, Bradley JM, Yang YF, Keller KE, Acott TS. Mapping molecular differences and extracellular matrix gene expression in segmental outflow pathways of the human ocular trabecular meshwork. *PLoS One*. 2015;10(3):e0122483.
102. Toki MI, Cecchi F, Hembrough T, Syrigos KN, Rimm DL. Proof of the quantitative potential of immunofluorescence by mass spectrometry. *Lab Investig*. 2017;97(3):329–334.
103. Jonkman J, Brown CM, Wright GD, Anderson KI, North AJ. Tutorial: guidance for quantitative confocal microscopy. *Nat Protoc*. 2020;15(5):1585–1611.
104. Tsukamoto T, Kajiwara K, Nada S, Okada M. Src mediates TGF-β-induced intraocular pressure elevation in glaucoma. *J Cell Physiol*. 2019;234(2):1730–1744.
105. Junglas B, Yu AHL, Welge-Lüssen U, Tamm ER, Fuchshofer R. Connective tissue growth factor induces extracellular matrix deposition in human trabecular meshwork cells. *Exp Eye Res*. 2009;88(6):1065–1075.
106. Tripathi RC, Li J, Chan WFA, Tripathi BJ. Aqueous humor in glaucomatous eyes contains an increased level of TGF-β2. *Exp Eye Res*. 1994;59(6):723–728.
107. Niu J, Li Z. The roles of integrin $\alpha v\beta 6$ in cancer. *Cancer Lett*. 2017;403:128–137.
108. McCarty JH. $\alpha v\beta 8$ integrin adhesion and signaling pathways in development, physiology and disease. *J Cell Sci*. 2020;133(12):jcs239434.
109. Katoh D, Nagaharu K, Shimojo N, et al. Binding of $\alpha v\beta 1$ and $\alpha v\beta 6$ integrins to tenascin-C induces epithelial-mesenchymal transition-like change of breast cancer cells. *Oncogenesis*. 2013;2(8):e65.
110. Fontana L, Chen Y, Prijatelj P, et al. Fibronectin is required for integrin alphavbeta6-mediated activation of latent TGF-beta complexes containing LTBP-1. *FASEB J*. 2005;19(13):1798–1808.
111. Zhong Y, Wang J, Luo X. Integrins in trabecular meshwork and optic nerve head: possible association with the pathogenesis of glaucoma. *Biomed Res Int*. 2013;2013:202905.

Investigative Ophthalmology & Visual Science

112. Lo HP, Nixon SJ, Hall TE, et al. The caveolin-Cavin system plays a conserved and critical role in mechanoprotection of skeletal muscle. *J Cell Biol*. 2015;210(5):833–849.
113. Burridge K, Wennerberg, K. Rho and Rac take center stage. *Cell*. 2004;116(2):167–179.
114. Keller KE, Bradley JM, Sun YY, Yang YF, Acott TS. Tunneling nanotubes are novel cellular structures that communicate signals between trabecular meshwork cells. *Investig Ophthalmol Vis Sci*. 2017;58(12):5298–5307.
115. Webber HC, Bermudez JY, Millar JC, Mao W, Clark AF. The role of Wnt / b -catenin signaling and K-cadherin in the regulation of intraocular pressure. *Invest Ophthalmol Vis Sci*. 2018;59:1454–1466.
116. Hirata E, Yukinaga H, Kamioka Y, et al. In vivo fluorescence resonance energy transfer imaging reveals differential activation of Rho-family GTPases in glioblastoma cell invasion. *J Cell Sci*. 2012;125(4):858–868.
117. Liesenborghs I, Eijssen LMT, Kutmon M, et al. The molecular processes in the trabecular meshwork after exposure to corticosteroids and in corticosteroid-induced ocular hypertension. *Invest Ophthalmol Vis Sci*. 2020;61(4):24.
118. Raghunathan VK, Thomasy SM, Strøm P, et al. Tissue and cellular biomechanics during corneal wound injury and repair. *Acta Biomater*. 2017;58:291–301.
119. Rubin J, Schwartz Z, Boyan BD, et al. Caveolin-1 knockout mice have increased bone size and stiffness. *J Bone Miner Res*. 2007;22(9):1408–1418.
120. Oh MJ, Zhang C, Lemaster E, et al. Oxidized LDL signals through Rho-GTpase to induce endothelial cell stiffening and promote capillary formation. *J Lipid Res*. 2016;57(5):791–808.
121. Bordeleau F, Lapierre ME, Sheng Y, Marceau N. Keratin 8/18 regulation of cell stiffness-extracellular matrix interplay through modulation of rho-mediated actin cytoskeleton dynamics. *PLoS One*. 2012;7(6):e38780.
122. Huveneers S, Daemen MJAP, Hordijk PL. Between Rho(k) and a hard place: the relation between vessel wall stiffness, endothelial contractility, and cardiovascular disease. *Circ Res*. 2015;116(5):895–908.

Investigative Ophthalmology & Visual Science